JPRS-UMS-92-007
15 APRIL 1992

JPRS Report

Science & Technology

Central Eurasia: Materials Science

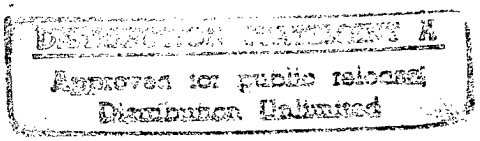

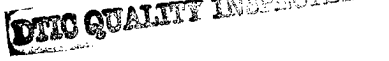

Science & Technology
Central Eurasia: Materials Science

JPRS-UMS-92-007

CONTENTS

15 APRIL 1992

Analysis, Testing

Coatings

Corrosion

Ferrous Metals

Nonferrous Metals, Alloys, Brazes, Solders

Nonmettallic Materials

Preparations

Treatments

Welding, Brazing, Soldering

Fracture Characteristics of Steel 24, Steel Kh18N10T Clad Metal Produced by Explosion Welding

927D0116A Kiev METALLOFIZIKA in Russian Vol 13 No 11, Nov 91 pp 3-8

[Article by I. Buchvarov, L. O. Zvorykin, Yu. Ya. Meshkov, S. Farforova, V. M. Falchenko, A. V. Shevchenko, Institute of Physics of Metals at the Ukrainian Academy of Sciences, Kiev, and Metal Science and Metal Technology Institute at the Bulgarian Academy of Sciences, Sofia; UDC 539.4]

[Abstract] The fracture patterns of the clad metal pair from steel 45 and steel Kh18N10T is examined from the viewpoint of a microspalling model which makes it possible to link the structural characteristics of the metal and its mechanical properties by means of quantitative criteria and to use a number of theoretical conclusions for analyzing and calculating for loading reliability of metal structures. The effort is aimed at establishing the fracture micromechanism of clad metals produced by explosion welding within a broad temperature range and examining the role of the structure as the principal factor controlling the level of the two most important mechanical features: the brittle failure strength referred to as the microspalling resistance and the toughness margin; it is shown that the tearing stress in the contact zone is an important feature for estimating the clad metal quality. The results show that the brittle failure process is controlled by the ferritic-pearlitic structure of steel 45, making it necessary to analyze, and search for, ways of optimizing this structural state since under today's treatment conditions, steel Kh18NJ10T has higher physical and mechanical properties; the results also show that the brittle strength level of clad metal is determined by the ferrite grain size of steel 45. Figures 3; references 2.

Strain Channels Under Electrically Stimulated Drawing Conditions

927D0116B Kiev METALLOFIZIKA in Russian Vol 13 No 11, Nov 91 pp 9-13

[Article by V. Ye. Gromov, V. Ye. Panin, V. Ye. Kozlov, Yu. F. Ivanov, Yu. P. Shkarkeyev, G. V. Pushkarev, Strength Physics and Metal Science Institute at the Siberian Branch of the USSR Academy of Sciences, Tomsk, and Siberian Metallurgical Institute, Novokuznetsk; UDC 669.71:539.382.2]

[Abstract] The origin of the ferritic steel loss of strength is examined by statistically analyzing the parameters of the substructure forming during regular and electrically stimulated strain and recorded by a diffraction electron microscope study; to this end, an attempt is made to clarify the cause of the low carbon steel plasticization. Welding wire from steel 08G2S (GOST 2246—70) annealed at 680°C for 10 hours and subjected to electrically stimulated (ESV) and conventional (OV) drawing at a 0.34 m/s rate with a total reduction of up to 64 percent is used in the study which reveals the presence of localized strain areas. The microstructure parameters of the strain channels are summarized under both types of strain and the dependence of the volume fraction of strain channels on the percent reduction is plotted. Variations in the number of mean transverse and longitudinal dimensions of the strain channels, the number of reflexes on the diffraction ring, and the angles of azimuthal and discrete disorientation with strain are calculated. The study shows that electrically stimulated drawing is a multifactorial process. Figures 2; tables 2; references 13: 12 Russian, 1 Western.

Strain Substructure and Reorientation Mechanism in High-Strength Nb- and V-Based Alloys With Disperse Hardening

927D0116C Kiev METALLOFIZIKA in Russian Vol 13 No 11, Nov 91 pp 14-20

[Article by A. N. Tyumentsev, V. Ch. Gonchikov, A. D. Korotayev, Siberian Engineering Physics Institute, Tomsk; UDC 669.018.4:541.451]

[Abstract] Using the electron microscope analysis method (FIZIKA METALLOV I METALLOVEDENIYE Vol 63 No 3, 1987, p. 598), the characteristic substructure developing with an increase in the strain in a Nb- or V-based alloy with superfine ZrO_2 particles ($2R \leq 10$ nm) is examined; in addition, certain new substructural elements developing as a result of the plastic reaction of high nonuniform stresses in the substructure with an unusually high crystal lattice curvature of up to one rad/μm are analyzed on the basis of the internally oxidized vanadium alloy of a similar type. The study demonstrates that the superfine particles effectively suppress the dislocation stress relaxation as a result of which the new substructure type is formed. The plastic relaxation characteristics of the high nonuniform stresses forming in this case are examined. The formation of the disorientation boundaries of a slanted type is discovered and attributed either to the difference in the edge and screw dislocation component mobility and proclivity for dislocation stress relaxation or to the diffusive mass transfer due to the drift of nonequilibrium point defects in the high local normal stress gradient fields. Figures 3; references 11.

Effect of Soluble Impurities on Amorphous $Fe_{85}B_{15}$ Alloy Solidification

927D0116D Kiev METALLOFIZIKA in Russian Vol 13 No 11, Nov 91 pp 44-48

[Article by V. V. Maslov, D. Yu. Paderno, Ye. A. Shishkin, O. Yu. Shvedkov, Institute of Physics of Metals at the Ukrainian Academy of Sciences, Kiev; UDC 539.213:669.15]

[Abstract] The effect of small additions of soluble impurities on the solidification of the $Fe_{85}B_{15}$ hypoeutectic alloy is studied. $(Fe_{0.99}M_{0.01})_{85}B_{15}$ alloys where M≡Ni, Co, Cr, Nb, Mo, or Re—transition metals characterized

by different surface activity relative to molten iron—are examined. To this end, amorphous 18-22 μm thick, 12-17 mm wide bands are produced by the rapid melt spinning method. It is shown that compared to the base alloy, the temperature of the onset of α-crystal precipitation from the amorphous matrix increases due to the presence of these impurities with a distribution coefficient in iron of <1 and drops somewhat in the presence of rhenium whose distribution coefficient is >1. No correlation with the surface activity of the impurity is found, making it possible to speculate that the effect of the impurities is manifested primarily not at the nucleation stage but during the crystal growth phase. The need for further studies of the crystallization process kinetics from the viewpoint of the thermal stability of amorphous alloys is stressed. Figures 1; tables 1; references 10.

Bulk Effects During Thermal Cycling of Invar Fe-Ni-Cr System Alloys

927D0116E Kiev METALLOFIZIKA in Russian Vol 13 No 11, Nov 91 pp 91-96

[Article by Yu. L. Rodionov, I. V. Starostenko, T. G. Shamilov, G. V. Shcherbedinskiy, G. V. Yudin, Central Scientific Research Institute of Ferrous Metallurgy; UDC 669.15'24]

[Abstract] A study of the dimensional change effect during the cooling and heating of Fe-Ni-Cr austenitic alloy samples as a function of the Ni and C content is reported and data on the structure of these alloys are cited. The study is prompted by the need for materials with a low thermal coefficient of linear expansion (TKLR) and a high level of mechanical properties. Alloys with 28-38 percent Ni and 0.1-1.0 percent C are smelted in an open induction furnace, diffusion-annealed, forged into rods, and water-quenched; samples for both dilatometry measurements in a Linseis instrument (Germany) and X-ray studies in a Geigerflex unit manufactured by the Rigaku Company (Japan) are then made from the rods. The carbon content is monitored radiographically. A standard FWHM software package is used for statistical processing of the findings. A model of the volume variation during the thermal cycling of carbon-containing Fe-Ni alloys is proposed; according to the model, there is a broad temperature range below the Curie point at which swelling processes occur while at the same time Invar Fe-Ni carbon containing alloys swell below a certain critical temperature (approximately 140°C). During the heating at a temperature above 140°C, the samples shrink. The reversible volume variation phenomenon assumes the greatest magnitude during the thermal cycle in the neighborhood of 140°C at certain Ni and C concentrations. Model versions describing the reversible volume change phenomenon which take into account the magnetostriction effects as well as the possible reversible C atom redistribution among octa- and tetrahedral interstitial sites are proposed. Figures 4; tables 1; references 9: 8 Russian, 1 Western.

Effect of Internal Macrostresses on Aging of Condensed Au-Co Films

927D0116F Kiev METALLOFIZIKA in Russian Vol 13 No 11, Nov 91 pp 112-115

[Article by A. T. Pugachev, D. B. Sikar, Scientific Research Institute of Precision Machine Building, Kharkov; UDC (669.21'25+539.216.2):539.26]

[Abstract] The characteristics of vacuum condensation deposited films are discussed and the effect of compressive and tensile macrostresses applied in the film plane on the decomposition of the supersaturated gold-cobalt solid solution is investigated. Two micrometer thick films deposited in a vacuum of at least 10^{-2} Pa by incomplete vaporization of a gold alloy with 1 percent Co and vapor condensation onto silver and molybdenum substrates at a 10 nm/s rate at 250°C are used in the study. An X-ray diffraction analysis established that in the initial state, the films represent a supersaturated single-phase substitution solid solution of Co in Au. An expression is derived for calculating the internal macrostresses in the films as a function of the Poisson coefficient and Young modulus; the theoretical values are consistent with the experimental results. The (420) line profiles of Au-Co film Co$K_{\alpha 1}$ after one and six months of storage are calculated. The microstructure of the Au-Co film after six months of storage at room temperature is examined under an electron microscope. An expression is derived for the motive force of the aging process as a function of the free energy of the initial and newly-developing phases; it shows that for the transformations accompanied by an increase in the specific volume, the work determined by the compressive macrostresses decreases the aging motive force while that determined by the tensile stresses—increases it. Figures 1; tables 2; references 6.

Investigation of Au Film Surface Morphology in Nanometer Band Using Scanning Tunnel Microscopy

927D0116G Kiev METALLOFIZIKA in Russian Vol 13 No 11, Nov 91 pp 116-119

[Article by I. V. Lyubinetskiy, P. V. Melnik, N. G. Nakhodkin, Kiev State University; UDC 537.533]

[Abstract] The effect of the morphology and surface roughness of metal films on their physical properties and the need for directly recording the surface microtopology are discussed; the scanning tunnel microscopy method (STM) which makes it possible to produce surface images in various media in real space with a resolution on the order of atomic dimensions along any of the three coordinates is used for investigating the microrelief of the Au film surfaces. To this end, a 30-100 nm thick film is spray-deposited in a vacuum at a 10^{-6} pressure at room temperature onto chromium-plated glass ceramic mica cleavages. The topographic images are recorded in the air in a 0.4 nA tunnel current mode at a 0.3 V potential difference between the W point and the sample. The

study confirms the possibility of using the scanning tunnel microscopy method for detailed studies of the characteristic features of the surface topology in the air within a 1,000-0.1 nm range. It is also established for the first time with the help of the scanning tunnel microscopy method for polycrystalline gold films that the microstructure of individual grain is determined by the set of atomically smooth terraces separated by ledges of one or several microlayers. Figures 3; references 7: 1 Russian, 6 Western.

Behavior of $Fe_{85-x}Co_xB_{15}$ Amorphous Alloy Films After Heating and γ-Irradiation

927D0116H Kiev METALLOFIZIKA in Russian Vol 13 No 11, Nov 91 pp 123-125

[Article by V. V. Polotnyuk, T. V. Yefimova, A. M. Shalayev, V. M. Shkapa, Institute of Physics of Metals at the Ukrainian Academy of Sciences, Kiev; UDC 539.213]

[Abstract] The specific saturation magnetization, coercive force, magnetic permeability, and remanent magnetization of a series of amorphous $Fe_{85-x}Co_xB_{15}$ alloys where x=12, 15, 17, 21, and 25 percent at. are investigated in the initial state and after heating and irradiation. Amorphous alloys are produced by spinning 30 μm thick, 10 mm wide bands. The magnetic properties are examined by the ballistic method in 800 kA/m fields accurately within 1 percent; the magnetic permeability is measured in 8-8 x 10^3 kA/m fields. The samples are studied in the initial state as well as after annealing at 700°C for 15 min (in a crystalline state) and irradiation with γ-quanta at <50°C at 1.2 MeV. The dependence of the specific saturation magnetization σ_s, coercive force H_c, magnetic permeability μ, and remanent magnetization B_r of Fe-Co-B alloys on heat treatment and the irradiation dose is summarized; crystallization of amorphous alloys decreases μ and increases H_c and B_r. γ-irradiation of amorphous alloys has virtually no effect on the magnetic characteristics after crystallization but noticeably affects them in the amorphous state: H_c drops in all cases and μ and B_r increase, i.e., the irradiation improves the soft magnetic properties. The effect of γ-irradiation on the magnetic characteristics is attributed to the radiation-induced mobility of boron which may probably lead to a change in the configurational and chemical short-range order. Tables 1; references 2.

Low-Temperature Brittleness of Fe-Cr+5 Al Percent Alloys

927D0117D Moscow METALLOVEDENIYE I TERMICHESKAYA OBRABOTKA METALLOV in Russian No 9, Sep 91 pp 18-19

[Article by Yu. A. Kurapov, V. N. Minakov, N. D. Rudyk, Institute of Materials Science Problems at the Ukrainian Academy of Sciences; UDC 620.178.2:669.14'26'71]

[Abstract] The low toughness of corrosion-resistant ferritic Fe-Cr-Al alloys prompted an investigation of the effect of hot plastic working, the Cr concentration, and grain size on the low-temperature ductility of Fe-Cr+5 percent Al alloys. Commercial grade alloys smelted in an open induction furnace are used as the raw materials. The component concentration of three alloys—Kh15Yu5T, Kh27Yu5T, and Kh45Yu5T—is summarized, and the effect of the quenching reheat temperature on the conditional cold-shortness temperature, the dependence of the conditional cold-shortness temperature on the grain size, and the tendency to embrittlement of alloys with various grain sizes as a function of the Cr concentration are plotted. An analysis of the findings demonstrates that the grain size reduction (by whatever method) makes it possible to lower considerably the cold-shortness temperature of high-chromium Fe-Cr+5 percent Al alloys while an increase in these alloys' cold-shortness temperature with the grain size is described by the Hall-Patch law. The tendency of the Fe-Cr+5 percent Al alloys to embrittlement with an increase in the grain size becomes even more pronounced with an increase in the chromium concentration. Figures 3; tables 3; references 7.

Acoustic Nondestructive Testing of Rail Hardness

927D0122E Moscow IZVESTIYA VYSSHIKH UCHEBNYKH ZAVEDENIY: CHERNAYA METALLURGIYA in Russian No 10, Oct 91 pp 30-32

[Article by S. N. Kudrin, V. V. Kazakov, G. A. Chervov, N. A. Chelyshev, Siberian Metallurgical Institute; UDC 621.771.26:539.53:53.082.4]

[Abstract] The shortcomings of the coercive force measurement and magnetoacoustic-based methods for nondestructive testing of the rail hardness stipulated by the quality control requirements are discussed and the use of the acoustic method for this purpose is reported. A block diagram of the device for testing the acoustic properties of steel in the calibration and main sections is presented and the amplitude-frequency response, oscillation damping factor spectra of various types of rail samples, and the dependence of the oscillation damping factor on the rail flaw magnitude at various testing frequencies are plotted. The experiments demonstrate that the dependence of the acoustic parameters of steel M76 rails on the state of their material may be used to monitor the surface hardness by the behavior of the oscillation damping factor at a 1,250 Hz frequency; the method's resolution is higher than that of a Brinell hardness gauge with an optical indentation measurement. The use of the amplitude-frequency response (AChKh) method is inefficient due to the strong dependence of the acoustic emission amplitude on the impact excitation force. Figures 3; tables 1; references 7.

Investigation of Microstructure and Magnetic Properties of Anisotropic Magnets

927D0122J Moscow IZVESTIYA VYSSHIKH UCHEBNYKH ZAVEDENIY: CHERNAYA METALLURGIYA in Russian No 10, Oct 91 pp 71-74

[Article by M. N. Shipko, A. F. Sitnikov, B. N. Bogdan, A. S. Pomelnikova, V. N. Peretyatko, Siberian Metallurgical Institute; UDC 669.018.58]

[Abstract] The effect of the crystalline grains of prepared ferrite on the microstructure and magnetic properties of anisotropic magnets on the basis of $SrFe_{12}O_{19}$ produced by single-stage sintering and the processes which limit the anisotropic microstructure formation of these magnets are investigated. The magnets are synthesized by the single-stage "ceramic" technology from strontium carbonate and pure-for-analysis hematite (ChSA) as well as prepared $SrFe_{12}O_{19}$ ferrite powder with a grain size of 0.4-1.0 μm. The magnets are sintered in a 79.6 kA/m magnetic field and their phase composition and structural state features are examined by the nuclear γ-resonance spectroscopy method; the microstructure parameters are studied in an IBAS-1000 automatic analyzer and DRON-3 X-ray diffractometer. Metallographic and electron microscopy studies are carried out using standard procedures. The dependence of the mean crystal grain disorientation angle and mean crystal grain size on the synthesis temperature, the particle disorientation angle distribution during the ferrite sintering at various temperatures, and the dependence of the magnet's coercive force and disorientation angle on the $SrFe_{12}O_{19}$ ferrite addition concentration are plotted. The magnetic properties of anisotropic magnets as a function of the synthesis temperature and duration are summarized. A comparison of experimental data to the results of an X-ray structural analysis indicates that the highest level of magnetic properties is produced in magnets characterized by high homogeneity, low values of crystal grain disorientation angles, an insignificant crystal lattice strain, and a fine grain structure. Figures 4; tables 1; references 5.

Acoustic Emission Fracture Diagnostics of Polycrystalline Superhard Materials

927D0123F Kiev SVERKHTVERDYYE MATERIALY in Russian No 4 (73), Sep-Oct 91 pp 33-36

[Article by N. V. Novikov, O. G. Lysenko, L. N. Devin, Superhard Materials Institute at the Ukrainian Academy of Sciences, Kiev; UDC 620.179.14:621.9.025]

[Abstract] The advantages of the acoustic emission (AE) method for diagnosing the fracture of polycrystalline superhard materials, such as cutter tips, and the method's limitations in predicting sudden tip failures are discussed. The possibility of resolving this problem is considered and the effect of the transducer placement on the tip on the acoustic emission signal characteristics is examined. An optimum transducer placement on the cutting tool is found and substantiated. Acoustic emission signals generated during the crack propagation in cutter tips under loading in an impact testing machine and during turning at an increasing cutting depth are analyzed. The experimental findings attest that acoustic signals convey reliable information about crack propagation in superhard polycrystalline materials. The acoustic emission transducer developed as a result of the study makes it possible to examine the fracture mechanism of cutting tools which is useful for developing computer-aided systems for assessing the cutting tool tip reliability during turning. Figures 4; references 9: 8 Russian, 1 Western.

Properties of Plasma Jet Coats From Complex Al-Ti Oxide Powders

927D0114D Kiev POROSHKOVAYA METALLURGIYA in Russian No 1 (349), Jan 92 pp 49-51

[Article by I. N. Gorbatov, N. F. Seliverstov, Yu. D. Repkin, A. Ye. Terentyev, G. G. Galimov, Ye. V. Kofman, A. I. Sesikov, I. S. Martsenyuk, Institute of Materials Science Problems at the Ukrainian Academy of Sciences; UDC 621.687]

[Abstract] The use of Al_2O_3-based powder materials with an addition of TiO_2 for hardening parts of textile machines by plasma jet spraying in various countries is discussed, and the structure and properties of aluminum oxide powders alloyed with 3, 13, and 25 percent (by mass) of titanium dioxide (A3T, A13T, and A25T) and produced by an atomizing firing of initial compound suspensions as well as certain features of plasma jet sprayed coats made from these powders are investigated. A photographic analysis indicates that the concentration of the main 15-90 μm fraction in the original powder varies within 60-80 percent while a radiographic analysis shows that γ-Al_2O_3 and TiO_2 phases and traces of α-Al_2O_3 are present in the A3T, A13T, and A25T powders. The structure and properties of plasma-jet deposited coats are compared to those produced from the Swiss Plasma-Technik AG powders. Wear resistance tests of both domestic and imported powders make it possible to recommend Al_2O_3-TiO_2 system materials for hardening and rebuilding parts of textile machines, printing presses, gas generators, and casting fittings. Figures 1; tables 3; references 3.

Effect of High-Temperature Coatings on Structure of ZhS6K Alloys

927D0117E Moscow METALLOVEDENIYE I TERMICHESKAYA OBRABOTKA METALLOV in Russian No 9, Sep 91 pp 24-25

[Article by L. P. Yefimenkio, Silicate Chemistry Institute at the USSR Academy of Sciences; UDC 669.782+621.793]

[Abstract] The γ'-phase and carbide precipitation in the ZhS6K alloy after a four h exposure to a 1,050-1,200°C temperature prompted a study of the composition and structure of the ZhS6K alloy after an application of the temperature resistant coat of 59.5 percent NiAl+30 percent Cr+5 percent W+5 percent Si+0.5 percent C onto its surface and subsequent extended exposure to a high temperature. The coat is produced by the powder-roasting method at 1,200°C for 10 minutes in a vacuum furnace at a residual pressure of $<133x10^{-3}$ Pa; the coat thickness varies within 200-300 μm. The element distribution in the ZhS6K alloy is examined by local X-ray spectral analysis in a Camebax and under a reflected electron microscope in Si *K* and Mo *L* radiation. The silicon distribution in the ZhS6K alloy phases after an additional heat treatment with various exposures is plotted. The conclusion is drawn that the diffusion of the coat elements in the Ni-based ZhS6K alloy greatly modifies its composition and structure to a considerable depth and that additional heat treatment worsens the properties of high-temperature coatings due to the icicular secondary phase precipitation throughout the alloy. Silicon diffusing into the alloy from the coating is concentrated not in the matrix but in the icicular phase, facilitating its precipitation and negatively affecting the coat properties. Figures 2; tables 1; references 5.

Investigation of Corrosion and Electrochemical Behavior of Steel Kh20N20 With Various Phosphorus and Silicon Concentrations in Nitric Acid Media

927D0137A Moscow ZASHCHITA METALLOV in Russian Vol 27 No 5, Sep-Oct 91 pp 726-736

[Article by O. V. Kasparova, V.Chigal, V. M. Milman, I. Kashova, S. D. Bogolyubskiy, N. M. Ostrikova, Scientific Research Physical-Chemical Institute imeni L. Ya. Karpov, Moscow, State Scientific Research Institute of Materials Protection imeni G. V. Akimov, Prague, Central Scientific Research Institute of Ferrous Metallurgy imeni I. P. Bardin, Moscow; UDC 620.193.41]

[Abstract] The negative impact of the phosphorus and silicon impurity segregation along the grain boundaries of austenitic stainless steels on their intercrystalline corrosion (MKK) in oxidizing media is discussed, and studies of the effect of silicon impurities and alloying additions on the corrosion and electrochemical behavior of hardened steel Kh20N20 with various phosphorus concentrations in nitric acid media (*Zashchita metallov* Vol. 18 No. 3, 1892, p. 336) are continued. To this end, the several and joint effect of phosphorus and silicon at a concentration of up to 0.1 and 5 percent, respectively, in a 27, 65, and 98 percent HNO_3 solution as well as a 27 percent solution containing 4 and 40 g/l Cr^{6+} is investigated. Samples from 15 smeltings are used in the experiment. The method of thermal etching in a vacuum is used to assess the effect of these elements on the relative free energy of the grain boundaries. Interference patterns of the etched surfaces and the cathode and anode polarization curves of steel in various nitric solutions are plotted. A study of the steel tendency toward intercrystalline corrosion and structural analyses indicate that the chemical composition of the intercrystalline zones and the content and structure of the oxide films forming on the steel surface, rather than the grain boundary energy, are the principal factors determining the metals' corrosion resistance in general and their intercrystalline corrosion resistance in particular. Figures 9; tables 1; references 16: 5 Russian, 11 Western.

Structure and Corrosion Resistance of Fe-Cr-Ni-Mo Maraging Steels

927D0137B Moscow ZASHCHITA METALLOV in Russian Vol 27 No 5, Sep-Oct 91 pp 737-742

[Article by V. V. Berezovskaya, N. V. Zvigintsev, M. S. Khaldyyev, Urals Polytechnic Institute; UDC 669.15.018:539.4:624.014]

[Abstract] The link between the structure and corrosion resistance of Fe-Cr-Ni-based maraging steels alloyed with molybdenum, titanium, and copper is investigated in samples after vacuum induction refining and diffusion annealing at 1,150°, hot rolling, water quenching at 950°, and aging at 450-750°. The chemical content, phase composition, and corrosion resistance of steels 03Kh11N10M2T and 03Kh11N10M2DT are summarized. The samples are examined in a 30, 75, and 90 percent H_2SO_4 solution. The study shows that as the sulfuric acid concentration increases, passivation of maraging steels of various contents is generally facilitated due to the strengthening of oxidative properties and that the corrosion resistance of Fe-Cr-N-Mo maraging steels in a nonoxidizing acidic medium is determined by the degree of solid solution separation with respect to Cr, making it undesirable to use low-temperature aging which leads to an intense Cr redistribution in the α-solid solution. On the other hand, the steel properties in an oxidizing medium are determined by the protective oxide film characteristics and the related alloying-passivating element redistribution, primarily molybdenum. The use of high-temperature tempering accompanied by the molybdenum redistribution among the α- and γ-phases is not suggested under such operating conditions. It is shown that steel alloying with copper reinforces the negative effect of the nonuniform molybdenum distribution in an oxidizing medium. Figures 2; tables 2; references 13: 11 Russian, 2 Western.

On Conjoint Effect of Boron and Silicon on Intercrystalline Corrosion in Steel Kh20N20

927D0137C Moscow ZASHCHITA METALLOV in Russian Vol 27 No 5, Sep-Oct 91 pp 743-752

[Article by V. M. Milman, O. V. Kasparova, Scientific Research Physical-Chemical Institute imeni L. Ya. Karpov, Moscow; UDC 620.196]

[Abstract] The intercrystalline corrosion-enhancing property imparted by microadditions of boron to stainless austenitic steel in highly oxidizing media and the intercrystalline corrosion-inhibiting influence of silicon as well as the effect of heat treatment conditions are discussed; the conjoint effect of boron and silicon additions on the intercrystalline corrosion of steel Kh20N20 in various structural states in both slightly and highly oxidizing media is investigated. Sheet samples of boron-containing steel Kh20N20 with a varying silicon concentration is studied in a tempered and hardened state in boiling HNO_3 solutions of various concentrations with four and 40 g/l of Cr^{6+}. An analysis reveals that in weakly oxidizing media, silicon has an ambiguous effect on the intercrystalline corrosion tendency of steel while in boiling 65 percent HNO_3 solutions at a potential corresponding to a transition from the passive to the transpassive state, Si enhances the intercrystalline corrosion tendency of tempered steel. In highly oxidizing media in the overpassivation area, an addition of $\geq$2.6 percent Si to B-containing steel completely suppresses its intercrystalline corrosion tendency in the hardened state. The authors are grateful to Academician Ya. M. Kolotyrkin for valuable advice. Figures 5; tables 5; references 34: 18 Russian, 16 Western.

Inhibiting Oxygen Corrosion of Copper in Water by Nitrogen-Containing Surfactants

927D0137D Moscow ZASHCHITA METALLOV in Russian Vol 27 No 5, Sep-Oct 91 pp 760-766

[Article by L. K. Khvatova, A. A. Abramzon, A. M. Sukhotin, Leningrad Technological Institute named after the Leningrad City Council; UDC 620.197.3]

[Abstract] The use of nitrogen-containing surfactants (PAV), primarily heteroaromatic compounds containing nitrogen in a five-membered ring, such as benzotriazole (BTA), for protecting copper from oxygen corrosion is discussed, and the inhibiting properties and absorption of several nitrogen-containing surfactants are examined at 60° on one μm copper layer vacuum-deposited on a glass ceramic plate. The studies demonstrate that due to being adsorbed on copper, the surfactants are capable of both inhibiting and enhancing its dissolution whereby the surfactants themselves are adsorbed either in a single layer or in many layers. Efficient surfactants capable of retarding copper corrosion in water have a high adsorption ability and are characterized by multilayer adsorption; they interact with copper ions forming stable chelate compounds whose isothermal curves are distinguished by a clear plateau. The effect of the solution pH on the surfactant's inhibiting ability and absorption is examined and the longevity of copper-surfactant films is investigated. It is shown that to be effective, an aqueous medium in which copper products operate must always contain dissolved surfactants. Figures 4; tables 2; references 18: 7 Russian, 11 Western.

Atmospheric Metal Corrosion Rate as Function of Time. III. Quantitative Dependence of Corrosion Resistance of Steels on Their Chemical Composition in Tropical and Temperate Climatic Regions

927D0137E Moscow ZASHCHITA METALLOV in Russian Vol 27 No 5, Sep-Oct 91 pp 789-798

[Article by Vu Dinh Vuy, Vietnamese National Center of Scientific Research, Tropical Technology Institute, Hanoi, and Physical Chemistry Institute at the USSR Academy of Sciences; UDC 620.193.2]

[Abstract] The need for mathematical equations expressing the dependence during certain timespans of the metal corrosion mass loss on the concentration of principal alloying elements in tropical regions is recognized, and a search for multifactorial empirical equations which make it possible adequately to describe the dependence of the initial corrosion rate on the active surface, the passivating properties of the corrosion product films, the corrosion resistance, and corrosion losses of mass by iron and various types of steel on their chemical composition under tropical and moderate conditions is reported. Test data accumulated for 11 types of steel and iron over a 16 year period in Panama and for 19 types of steel over three years in Czechoslovakia are used in the study. It is shown on the basis of 30 multiple regression equations derived by Burda, Southwell, and Bultman that all steel components have a complex effect on the initial atmospheric corrosion rate, passivating properties of the corrosion products, and mass losses due to corrosion as a function of their concentration, the presence of other elements, atmospheric conditions, and exposure. The analyses are performed on an IBM PC XT/AT microcomputer using standard software. Ni, V, Cu, Si, S, Mn, P, and C generally increase the passivating properties of corrosion products, Mo decreases the passivating properties in the semiurban and maritime tropical environment, Cr increases the passivating properties and corrosion resistance in semiurban and maritime tropical environments but decreases them in temperate regions with contaminated air. The degree and mechanism of the effect of individual chemical elements in steel on the initial corrosion rate, passivating properties of corrosion products, and corrosion resistance will be examined in the next report. The author is grateful to Prof. Yu. N. Mikhaylovskiy for useful discussions. Tables 8; references 10: 3 Russian, 7 Western.

Physicochemical Simulation of Metal Corrosion in Seawater

927D0137F Moscow ZASHCHITA METALLOV in Russian Vol 27 No 5, Sep-Oct 91 pp 799-803

[Article by B. B. Chernov, S. A, Ponomarenko, Physical Chemistry Institute at the USSR Academy of Sciences and Far Eastern Corrosion Station; UDC 620.193.27]

[Abstract] The inhibiting effect of poorly soluble compound deposition on metals in seawater on their corrosion is discussed, and kinetic corrosion rate equations derived on the basis of general physicochemical protective film development patterns are used to predict the corrosion behavior in seawater; in so doing, the unknown quantities are determined from available results of corrosion tests. It is assumed that at any moment, the time derivative of the corrosion depth is inversely proportionate to the deposited product thickness, i.e., is determined by the mass transfer through the layer. A statistical analysis is used to assess the effect of the seawater temperature and oxygen concentration on the permeability of corrosion products and steady-state corrosion rate, and it is demonstrated that the model makes it possible to predict the corrosion of low-alloyed steels from data of physicochemical seawater analyses accurately within +/-40 percent and the copper corrosion with a +/-47 percent spread. Tables 1; references 12: 11 Russian, 1 Western.

Aluminum Softening and Embrittlement in Salt Melts

927D0137G Moscow ZASHCHITA METALLOV in Russian Vol 27 No 5, Sep-Oct 91 pp 804-809

[Article by A. A. Barkov, Physical Chemistry Institute at the USSR Academy of Sciences; UDC 620.193.43]

[Abstract] The mechanical and electrochemical behavior of aluminum in molten salts are investigated; to this end, cylindrical aluminum samples of a 99.997 percent purity are tested at a constant 2 percent min^{-1} straining rate with a +/-2° temperature control; the anode current behavior during plastic deformation under potentiostatic conditions in KCl-LiCl melts with various KNO_3 concentrations, and the effect of KNO_3 additions in the KCl-LiCl melt on the aluminum anode dissolution current rise and elongation at rupture are examined and plotted. The study reveals a high mechanical and electrochemical effect of potentiostatic aluminum polarization in a chloride melt at 400° which is interesting from an electrochemical strain measurement viewpoint; a transition from ductile to brittle failure and back in strained aluminum is discovered with an addition of potassium nitrate to the chloride melt at 400°; it is shown that aluminum may become ductile either due to an increase in the oxide film dissolution rate or as a result of a pitting repassivation acceleration. Figures 3; references 6: 2 Russian, 4 Western.

On Protective Ability of Hydroxide Layers Forming on Iron Surface in Bichromate Solution in Presence of Titanium or Zirconium Salts

927D0137H Moscow ZASHCHITA METALLOV in Russian Vol 27 No 5, Sep-Oct 91 pp 814-818

[Article by N. B. Lukina, A. I. Marshakov, Physical Chemistry Institute at the USSR Academy of Sciences; UDC 620.198]

[Abstract] The factors which enhance the iron dissolution rate during the reduction of oxygen-containing oxidants, including bichromate ions, are discussed, and the protective ability of the films forming on the surface of iron during its corrosion in a bichromate solution in the presence of titanyl and zirconyl ions is investigated. To this end, the iron sample (St3) corrosion rate is measured by the mass loss. The coats are produced by exposing the samples to 10 and 30 min in 0.05 and 0.5 M solutions of sulfuric acid, sodium sulfate, potassium bichromate, and Zr and Ti sulfates. The dependence of the iron electrode corrosion current on the bichromate concentration during the coat deposition and the dependence of the iron electrode corrosion current on the bichromate concentration during corrosion tests are plotted, and the results of corrosion tests are summarized. An analysis indicates that an addition of Ti^{4+} or Zr^{4+} ions to bichromate solutions improves the protective properties of the resulting conversion films and that the iron corrosion process in oxidizing media may be inhibited by adding cations of metals characterized by a low pH of hydrate formation. Figures 3; tables 1; references 5.

On Base Dissolution Patterns During Ni-Cr-Si-B Protective Coat Formation on Iron and Steel

927D0137I Moscow ZASHCHITA METALLOV in Russian Vol 27 No 5, Sep-Oct 91 pp 827-830

[Article by V. N. Filipovich, L. P. Yefimenko, Ye. A. Antonova. Silicate Chemistry Institute at the USSR Academy of Sciences; UDC 621.793]

[Abstract] Metal protection from high-temperature corrosion by applying slip-roasted coats, whereby the base metal actively participates in the coat formation process and dissolves partially in the coat melt, is discussed, and the dissolution kinetics and equilibration rate are investigated; in the steady-sate condition, the coat melt is in a quasiequilibrium with the base in regard to the metal concentration. A 1M coat consisting of 70 percent Ni, 20 percent Cr, 5 percent Si, and 5 percent B, by mass, is formed on steel 12 Kh18N9T and Armco iron while slip powders are prepared from the PNE-1 electrolytic nickel, PKhS chromium, KrO crystalline silicon, and amorphous boron. The samples are roasted for two to 30 minutes in a vacuum furnace at a residual pressure of under 10^{-3} mm Hg within a 1,060-1,200° range. An analysis made by a defocused electron beam probe shows that iron dissolved in the coat melt during the coat formation is distributed unevenly among the phases—solid solution, chromium borides, and eutectics—yet the iron content in each phase is virtually constant throughout the coat depth two minutes after the start of roasting. The possibility of controlling the coat deposition process and the coat thickness without affecting its protective properties is demonstrated. The results made it possible to optimize the coat deposition parameters for a large class of Ni-Cr-Si-B protective coats and significantly decrease the protected metal corrosion in the coat melt during the roasting. Figures 1; tables 2; references 8: 7 Russian, 1 Western.

Study of Corrosion Cracking of Steel in $HSiCl_3$ Synthesis Medium

927D0137J Moscow ZASHCHITA METALLOV in Russian Vol 27 No 5, Sep-Oct 91 pp 830-832

[Article by N. A. Bokshitskaya, I. D. Meshcheryakova, I. L. Kharina, N. Ye. Yermolayeva, M. A. Khotsernov, State Scientific Research Institute of Hetero-Organic Compound Chemistry and Technology; UDC 620.194]

[Abstract] Weld metal cracking in chemical synthesis reactors made from carbon steel 09G2S and stainless steels 12Kh18N10T and 10Kh17N13M2T prompted a study of complex-stressed samples—bottoms of three reactors—made from welded and seamless blanks by cold stamping in order to assess the effect of the process medium and welding, temperature, and thermal cycling stresses related to the reactor design and operating conditions on stress corrosion cracking of these steels. The investigation reveals that under isothermal conditions in the air, steels 09G2S and 12Kh18N10T do not crack while in the synthesis media of $HSiCl_3$-$SiCl_4$, corrosion cracking develops by the silicide-chloride mechanism due to the conjoint effect of the chlorosilanes and chlorides entering the medium together with the synthesis product during its hydrochlorination. Metallographic studies under a scanning electron microscope and electron beam microanalyses show that cracking is accompanied by the development of brittle peeling films of the Fe-Si solid solution with an unstable silicon concentration. The chloride systems also aggravate the

intercrystalline corrosion and pitting in stainless steel due to a selective grain boundary dissolution. References 5: 4 Russian, 1 Western.

Effect of Laser Treatment on Corrosion Resistance of Nickel-Plated Steel 10

927D0137K Moscow ZASHCHITA METALLOV in Russian Vol 27 No 5, Sep-Oct 91 pp 832-834

[Article by I. Yu. Khodyrevskaya, Ye. K. Vostrikova, Ye. S. Batkin, Energiya Scientific Production Association, Voronezh; UDC 621.791.72:621.373.826:620.178.311.868]

[Abstract] The changes in the physical and chemical properties of metal as a result of laser fusion or welding of parts with an inorganic coating, particularly the changes in their corrosion resistance due to the coat burnout and the mixing of the coat material with the base metal, is addressed, and the possibility of producing a corrosion-resistant welded joint of parts without an additional corrosion protection is investigated. To this end, the effect of laser burnoff of low-carbon steel 10 nickel-plated by chemical deposition on its resistance to amorphous corrosion is examined. The samples are burned off using a Kvant-15 laser unit with a 4 ms, 0.75-3.45 J pulse with a spot diameter of 0.6-0.8 mm, i.e., at a power density of 30-100 kW/cm^2, which ensures a 0.05-0.41 mm fusion depth. The polarization curves of bare and nickel-plated samples in a simulated pH 6 condensate atmosphere and the free corrosion potential behavior in the time domain are plotted. Under tests of atmospheric corrosion, bare samples displayed corrosion after two days while nickel-plated samples did not show corrosion even after 24 days. The results indicate that laser flashing of the surface of nickel-plated steel 10 alters the type of corrosion process in it and decreases the corrosion resistance only slightly and does not call for additional protection from atmospheric corrosion under commercial operating conditions. Figures 2; references 4.

Laser-Induced Electrodeposition of Ni on Cu From Sulfate Electrolyte

927D0137L Moscow ZASHCHITA METALLOV in Russian Vol 27 No 5, Sep-Oct 91 pp 853-855

[Article by Yu. V. Seryanov, M. V. Nesterenko; UDC 621.793.14]

[Abstract] Localized laser-stimulated electrolytic precipitation of nickel on copper for the purpose of producing the topology images of printed boards and microchips developed in the chemical copper etching solutions containing strong oxidants is investigated. The experimental unit, designed on the basis of an LTN-102 solid-state laser, has a λ=1.06 μm radiation with a $\leq$125 W power; the electrolyte used for electrolytic precipitation of nickel and the electrolytic cell design are described. Cathode potentiostatic curves of nickel deposition on a copper foil, the dependence of the deposition current density and acceleration coefficient on the radiant intensity, and the theoretical radial-velocity distribution of the local line width during the laser-stimulated electrolytic precipitation of nickel on metallized aluminum oxide ceramics are plotted. The findings reveal that the optimum potential of laser-induced electrodeposition of nickel is -0.88 V and the optimum radiation density is 21 kW/cm^2. The coat thickness decreases with an increase in the relative distance from the line center to the radius of the focused laser beam and decreases sharply given rr_o. The maximum resolution of the method may reach 108 lines/mm while the mean statistical irregularity may be decreased to 2.8 percent. It is demonstrated that laser-stimulated electrolytic nickel precipitation on copper may be used for making hybrid microwave-band integrated circuits and protecting them from corrosion by the subtractive method. Figures 3; references 7: 6 Russian, 1 Western.

Inhibition of Steel Corrosion During Acid Treatment of Carbonate Rock

927D0137M Moscow ZASHCHITA METALLOV in Russian Vol 27 No 5, Sep-Oct 91 pp 859-861

[Article by N. M. Gontmakher, V. P. Grigoryev, O. A. Ivashchenko, Ye. A. Skvortsov, S. V. Myalkovskiy, P. S. Shmelev, Scientific Research Institute of Physical and Organic Chemistry and Rostov State University; UDC 621.197.3]

[Abstract] Hydrochloric acid treatment of wells in a number of deposits, including the Astrakhan Gas Condensate Deposit (AGKM), and the shortage of imported inhibitors prompted an attempt to develop and implement easily accessible and inexpensive inhibitors manufactured on the basis of large-scale byproducts of the gas and petroleum refining industry. Corrosion measurements are taken on domestic steel "Category II Drilling D" and imported steels C-75, SM90SSU, and C-95 used at the Astrakhan Gas Condensate Deposit; to this end, samples are scraped, degreased, and exposed to P_2O_5 in an exiccator to stabilize the surface. In addition, samples of oil quenched steel 40Kh are tested for corrosion cracking (KR) under uniaxial tension and samples of annealed steel 20 are tested for low-cycle fatigue. Devanathan's method with an IPT-1 coulometric integrator is used to measure the hydrogen diffusion through a steel membrane. The corrosion rate of steels SM90SSU and C-75 in solutions with various HCl concentrations and an RGU-2 inhibitor and the corrosion rate of the C-75 and D steel in a 15 percent HCl with various types of inhibitors are summarized; cathode and anode polarization curves are plotted for steel D without an inhibitor and with various inhibitors. The results make it possible to estimate the efficiency of these inhibitors in retarding hydrogen diffusion through a steel membrane in a hydrochloric acid solution constantly saturated with hydrogen sulfide; the RGU-AN+OP-7 is found to be the most effective for this purpose; moreover, the RGU-2 and RGU-AN, especially with OP-7, are effective in

retarding the cathodic and anodic reactions. These inhibitors are being commercially produced at the Azot Production Association at a cost of 600 rubles per ton. Figures 1; tables 3; references 6: 5 Russian, 1 Western.

On Ways of Improving Volatile Atmospheric Corrosion Inhibitor Efficiency

927D0137N Moscow ZASHCHITA METALLOV in Russian Vol 27 No 5, Sep-Oct 91 pp 864-867

[Article by E. M. Agres, Leningrad Petrochemistry Production Association; UDC 620.197.3]

[Abstract] The efficiency criterion of volatile inhibitors of atmospheric corrosion is discussed and the specific case of inhibitor evaporation from the surface of a planar disc—a base of a cylinder whose other base is covered with a thin film of water—is considered. The dependence of the cyclohexylamine carbonate (KTsA) inhibitor diffusivity in the air on the external pressure at various degrees of rarefaction is plotted; an analysis of the diagram indicates that a decrease in the pressure in the system enhances the inhibitor activity while without the inhibitor, air evacuation alone does not retard the corrosion rate. It is suggested that in addition to reducing pressure, in order to increase the volatile inhibitor's efficiency inside hollow structures, it should be evenly distributed in small spherical gauze bags hung inside. Figures 1; tables 1; references 7.

TPI-4 as Atmospheric and Water Corrosion Inhibitor of Fe-C Alloys

927D0137O Moscow ZASHCHITA METALLOV in Russian Vol 27 No 5, Sep-Oct 91 pp 867-870

[Article by A. I. Trufanova, T. A. Lazareva, S. F. Khlebnikova, N. N. Voyevodina, Tula Polytechnic Institute; UDC 620.197.3]

[Abstract] The effect of oxynitroaromatic acid salts on the corrosion and electrochemical behavior of steel St3 in a lightly mineralized medium is discussed, and the efficiency of the nitro derivative-based TPI-4 inhibitor for Armco iron, steel St3, and pearlitic pig iron is investigated. To this end, the effect of potential on the incremental capacitance of iron electrodes and the anode and cathode polarization curves of the Fe-C alloys in a borate buffer solution are plotted, and the corrosion rate of steel, iron, and pig iron at various inhibitor concentrations is measured. The results show that the TPI-4 is a typical passivating inhibitor which is highly efficient under the free corrosion conditions in a 0.5 M sodium sulfate solution. The high efficiency of the TPI-4 inhibitor is also confirmed by a visual inspection of samples and products after accelerated corrosion tests in hot moisture and cold chambers. The inhibitor efficiency is due to the high adsorption ability of the organic complex with a hydrogen bond, the high depolarizing effect of the compounds containing nitro groups, and the ability of Fe-C alloy to revert to a passive state. Figures 2; tables 1; references 6.

On Development Trends in Domestic Steel-Making Industry

927D0115A Moscow STAL in Russian No 1, Jan 92 pp 20-24

[Article by O. V. Yuzov, Moscow Institute of Steel and Alloys; UDC 669.78]

[Abstract] Recent changes in the operating conditions in the national economy, especially in ferrous metallurgy, prompted a study of the principal development trends in the domestic steel-making industry and a comparison to the industry status and development trends in other countries. The steel output and production structure dynamics in the United States, Japan, the Federal Republic of Germany, France, Great Britain, and Italy in 1970, 1975, 1980, 1985, and 1989 are analyzed for the total steel production volume in general and oxygen-converter, open hearth, electrical sheet, and Thomas steel in particular and the ratio between the oxygen-converter and electric furnace smelted steel is calculated. The trend toward substituting open hearth and Thomas steel with oxygen-converter and electric furnace smelted steel is noted. Direct and total capital investments in the production of cast slabs of converter steel and cast electric furnace smelted steel in 1991-1995 are projected. The conclusion is drawn that the domestic steel-making industry needs a realistic retooling program in the light of the transition to a market economy; the almost insurmountable obstacles on the path toward retiring most of the largest open hearth plants by 2005 as well as the need considerably to lower the steel output level reached in the country must be taken into account in this program. It is suggested that converter steel smelting be brought to a level of 50 percent of the total volume, electric furnace steel—to 30 percent, and open hearth furnace steel—to 20 percent of the total. The following target figures are adopted for 2005: 70.0 million tons of converter steel, 35.0-40.0 million ton of electric furnace steel, and 25.0-30.0 million tons of open hearth steel. Tables 3; references 8.

Improving Conticast Steel Quality by Microalloying With Clad Powdered Inoculants

927D0115B Moscow STAL in Russian No 1, Jan 92 pp 24-27

[Article by B. F. Belov, G. A. Nikolayev, L. A. Poznyak, A. G. Shalimov, A. I. Trotsan, O. V. Nosochenko, V. G. Lenskiy, V. P. Kharchevnikov, Institute of Materials Sciences Problems at the Ukrainian Academy of Sciences, Azovstal Integrated Iron and Steel Works, Makeyevka Experimental Technical Design Office, and Central Scientific Research Institute of Ferrous Metallurgy; UDC 621.746.27.047]

[Abstract] Microalloying of steel with chemically active elements—the physical and chemical principles of ladle refining—is considered and the process of molten steel inoculation with clad powders (the PPM process) is examined in detail. The main features of the PPM process developed at the Institute of Materials Sciences Problems at the Ukrainian Academy of Sciences which include clad powdered modifiers of the band (L-PM) and wire (P-PM) type consisting of a solid core-filler and a metallic coating are summarized. The cladding is made from 0.3-0.5 mm thin coil steel 08kp or 08sp and the filler, from powdered components of chemically active elements, such as Al, Ti, B, Ca, Ba, alkali and rare earth metals, etc., and fluxes of a $\leq$2.0 mm fraction; the principal specifications of band- and powder-type inoculants are summarized and the method of feeding the band or wire into the intermediate ladle of the continuous casting machines (MNLZ) is outlined. The calcium assimilation by cerium for various inoculation techniques, the concentration of nonmetallic inclusions in continuously cast steel 09G2BT, and the concentration variation and segregation coefficient of elements in continuously 09G2S cast slabs as a function of the ladle refining method are summarized. An analysis shows that the PPM method is very efficient and increases the stability and assimilation of the inoculants as well as decreases their consumption. The equipment complex necessary for utilizing the method requires an outlay of about three rubles per ton and is reliable and simple to operate. The PPM process is also ecologically pure and improves working conditions. Figures 1; tables 4.

High-Quality Cold-Finished Vacuum-Treated Bearing Steel From 8.35 Ton Ingot

927D0115F Moscow STAL in Russian No 1, Jan 92 pp 72-74

[Article by G. I. Kaplanov, Ye. I. Yarovoy, I. N. Sigleyev, A. V. Malko, Ukrainian Scientific Research Institute of Specialty Steels; UDC 669.14.018.24-124.2]

[Abstract] The reasons for limiting the mass of the ingots for making bearing steels—mostly the stringent requirements imposed on the nonmetallic inclusion concentration and the macro- and microstructure—are discussed and a method of producing vacuum-treated cold-finished bearing steel with an up to 25 mm diameter in bundles weighing up to 1,000 kg for subsequent cold upsetting from 8.35 ton ingots made at the Cherepovets Integrated Iron and Steel Works (CherMK) is described. The smelting of steel ShKh15 in 100 ton arc furnaces for this purpose is outlined and the C, Si, Mn, and Cr content in three smeltings measured. The quality of ShKh15-V steel in 150x150 mm ingots, i.e., the concentration of nonmetallic inclusions, microporosity, structural striation, carbide segregation, central porosity, point inhomogeneity, and subshinking segregation, and the results of quality control of semi-finished rolled stock and cold-finished steel, are summarized. The tests confirm the expediency of nondecarburizing annealing of the rapidly cooled semi-finished rolled products in bell-type gas-fired furnaces with a shielding atmosphere without preliminary pickling. The new method makes it possible to make up to 87 percent of first quality bundles which meet the OST 14-19-147—85 requirements. Tables 4; references 8.

Effect of Nitrogen Additions on Aging of Low Carbon Austenitic Steel 0Kh17N14M3G2

927D0117C Moscow METALLOVEDENIYE I TERMICHESKAYA OBRABOTKA METALLOV in Russian No 9, Sep 91 p 17

[Article by A. N. Zankov, V. A. Tsygvintsev; UDC 539.376:669.14.011.8]

[Abstract] The high intercrystalline corrosion resistance, an elevated creep resistance, and adequate strength of steel 0Kh17N14M3G2 with a 0.005 percent C and 0.007 percent or 0.22 percent N concentration which make it suitable for the nuclear power industry prompted an investigation of the phase transformations, lattice constants, and microstress in steel 0Kh17N14M3G2 after air quenching and aging under various conditions. To this end, tubular samples are treated by the solid-phase decarburization and nitrogen alloying and studied radiographically in an ADP-2 diffractometer in copper's *K* radiation. The results indicate that in corrosion-resistant austenitic steels, the effect of nitrogen is similar to that of carbon in the process of long-term aging, in that N also suppresses the σ-phase precipitation; furthermore, in steel 0Kh17N14M3G2 with an up to 0.2 percent N concentration and a low carbon content, the formation of phases during long-term aging is controlled by the Cr diffusion. Tables 1; references 5: 4 Russian, 1 Western.

Membrane Refining as Steel Deoxidation Method

927D0122A Moscow IZVESTIYA VYSSHIKH UCHEBNYKH ZAVEDENIY: CHERNAYA METALLURGIYA in Russian No 10, Oct 91 pp 1-5

[Article by V. Ye. Roshchin, A. A. Epov, V. P. Gribanov, Chelyabinsk Polytechnic Institute; UDC 669.046:669.054.7]

[Abstract] The use of membrane or septum for separating solutions, i.e., reverse osmosis, ultrafiltering, evaporation through a septum, dialysis, and electrodyalisis, is discussed and the use of electrodyalisis for deoxidizing and refining metals without an electric field application—under the effect of the oxygen concentration gradient on both side of the membrane—is considered. The effect of the external electric field on the oxygen transition through the membrane is analyzed, the deoxidation duration curves are plotted, and the experimental unit design is presented. The experiments demonstrate the possibility of refining a metallic melt through a solid electrolyte ceramic membrane with anion conductance, provided that the electric potential difference between the phases separated by the membrane is equalized. The results also show that the external electric field application does not significantly affect the oxygen removal rate yet considerably complicates the electrochemical cell design and leads to unproductive outlays of electric power. Figures 6; references 8: 7 Russian, 1 Western.

Temperature Distribution Through Reaction Zone Volume During Metal Blasting With Oxygen

927D0122B Moscow IZVESTIYA VYSSHIKH UCHEBNYKH ZAVEDENIY: CHERNAYA METALLURGIYA in Russian No 10, Oct 91 pp 15-18

[Article by V. I. Baptizmanskiy, Yu. S. Paniotov, A. Ye. Kupchinskiy, Dnepropetrovsk Metallurgical Institute; UDC 669.184]

[Abstract] The effect of the reaction zone temperature and its behavior during blasting on the course of the physical and chemical processes occurring during the converter smelting is discussed and an attempt experimentally to plot the temperature distribution throughout the reaction zone by the probing method with the help of consumable refractory indicator blocks is reported. To this end, quartz, Alundum, and compacted magnesite rods and slabs with a 1,973, 2,323, and 2,573K melting point, respectively, are used. The lab converter used in the experiment is described; the 1,973 and 2,573K isothermal curves are plotted during the blasting of low carbon metal with oxygen at various pressures and the temperature variation as a function of the relative volume of the reaction zone at various carbon concentrations in the bath is examined. The experimental temperature distribution in the reaction zone as a function of the carbon concentration in the metal can be described well by an exponential law. The reaction zone superheating relative to the peripheral bath sections is analyzed and temperature gradients are calculated; the latter attest to the dominant effect of convection on the heat exchange in the converter bath. Figures 2; tables 4; references 6.

Silicon Reduction Characteristics During Production of Its Alloys With Iron

927D0122C Moscow IZVESTIYA VYSSHIKH UCHEBNYKH ZAVEDENIY: CHERNAYA METALLURGIYA in Russian No 10, Oct 91 pp 20-23

[Article by N. V. Tolstoguzov, Siberian Metallurgical Institute; UDC 669.168]

[Abstract] The characteristic features of silica reduction during the smelting of Si-alloyed iron are discussed and constitution diagrams of the Si-O-C and Fe-Si-O-C systems are plotted; an analysis of the diagrams shows that under equilibrium conditions, the carbide breakdown and formation of the end product—silicon—occur due to a silicon carbide reaction with silicon monoxide. The method of optimal alloy smelting models is used to establish the peculiarities of silicon reduction; to this end, it is assumed that the ferroalloy furnace consists of three zones: low- and medium-temperature zones and a zone where the gaseous SiO concentration exceeds its equilibrium level while the condensed phases consist of three components—SiO_2, SiC, and Si. The effect of the silicon concentration on the amount of carbon necessary for capturing gaseous silicon monoxide is plotted; the results show that the amount of carbon necessary for

extracting silicon during the smelting of FS45, FS65, and FS90 ferrosilicon with the Kr0 silicon increases with an increase in the amount of gaseous SiO in the alloy from 10.5 percent for a 45 percent ferrosilicon alloy to 100 percent for melting crystalline silicon; a temperature increase in the hearth slightly improves the silicon melting conditions. Figures 3; figures 4.

Effect of Chemical Composition and Cooling Condition on Mechanical Properties of 09G2S Coil Steel

927D0122G Moscow IZVESTIYA VYSSHIKH UCHEBNYKH ZAVEDENIY: CHERNAYA METALLURGIYA in Russian No 10, Oct 91 pp 53-55

[Article by M. A. Shumilov, D. I. Yaroslavskiy, L. A. Zubotenko, Ye. D. Poberezhskaya, S. A. Skrynko, Mariupol Metallurgical Institute; UDC 669.15-194:621-413]

[Abstract] The dependence of the mechanical properties of 4 to 8 mm-thick rolled sheets from steel 09G2S on the variability of the chemical composition, the final rolling and coil winding temperature, and the microstructure is examined in order to ascertain the reason why coils of steel 90G2S fail to meet the GOST requirements. Statistical processing of the results of acceptance tests and chemical analyses by the method of correlation and regression analysis is used. The study demonstrates the possibility of increasing the strength of hot rolled sheets of steel 09G2S while ensuring the necessary impact strength and toughness by increasing its carbon equivalent C_e at the expense of manganese, silicon, titanium, and carbon. A decrease in the strength of the hot rolled sheet is usually accompanied by an increased concentration of structurally free ferrite. It is recommended that coils be wound at a temperature not exceeding 650°C in order to increase the sheet strength while maintaining the requisite GOST requirements imposed on the metal ductility and toughness. References 3.

Steel 08Kh18N10T Hardening by Disperse Particles During Explosion Alloying

927D0122I Moscow IZVESTIYA VYSSHIKH UCHEBNYKH ZAVEDENIY: CHERNAYA METALLURGIYA in Russian No 10, Oct 91 pp 60-63

[Article by V. F. Nozdrin, S. I. Gubenko, S. M. Usherenko, Dnepropetrovsk Metallurgical Institute; UDC 669.046:534.2:621.385.833]

[Abstract] The method of explosion alloying in order to harden metallic materials with microfibers and hard disperse particles and change the physical and mechanical properties of the metal is discussed and the structural changes occurring in austenitic steel 08Kh18N10T during the explosion alloying as well as the factors responsible for hardening are investigated. Hot rolled steel strip samples are annealed in a vacuum at a 1,200°C temperature for two hours in order to relieve the taut strained state. Nickel and titanium cyanide particles of the 40-125 μm fraction are used as projectiles. The samples' microstructure before and after the explosion alloying treatment are examined under a Nanolab-7 scanning electron microscope and EMB-100B transmission electron microscope. An analysis demonstrates that the hardening of the steel matrix by disperse particles at a 15 GPa pressure and a two km/s velocity is a multifactorial process: the particles themselves facilitate the hardening of steel by serving as an obstacle of the crystal lattice defect migration and by generating secant stress fields around them while channel and channel zones have a reinforcing effect. The local zone amorphization and microalloying near the channel walls also contribute to hardening; moreover, rapid plastic deformation of austenite and polymorphous transformations induce the strain hardening of steel. All of these factors are concurrent, so the hardening effect is determined by their composite action. Figures 2; references 11: 10 Russian, 1 Western.

Approximate Estimate of Single Crystal Nickel-Based Superalloy Density

927D0117F Moscow METALLOVEDENIYE I TERMICHESKAYA OBRABOTKA METALLOV in Russian No 9, Sep 91 pp 25-27

[Article by N. V. Petrushin, I. A. Ignatova, L. A. Dyachkova, All-Union Aviation Materials Institute; UDC 620.192.47:669.245]

[Abstract] The dependence of the density of single crystal nickel-based CMSX-2, PWA 1480, NASA IR-100, 203E, RN4, RRSR99, MXON, RR2000, TMS-1, and AM3 superalloys on their chemical composition is summarized on the basis of published foreign and domestic data; the study is prompted by efforts to increase the long-term strength of superalloys by alloying them with an element having a large atomic weight, e.g., tungsten, tantalum, rhenium, and molybdenum, which often have a negative effect of increasing the mass of the product. As a result, an attempt is made to derive an analytical dependence of the alloy density on the alloying element concentration in order to predict the alloy density and use it as the optimization variable for developing high-temperature nickel alloys. A formula connecting the alloy density to the mean atomic mass of the alloy and lattice cell volume is derived, and a comparison to experimental data shows that it is accurate within 1.2 percent. Tables 2; references 9: 2 Russian, 7 Western.

Antifriction Properties of Aluminum Alloys After Surface Laser Alloys

927D0118G Moscow METALLOVEDENIYE in Russian No 10, Oct 91 pp 34-36

[Article by Ya. D. Kogan, Z. S. Sazonova, V. D. Aleksandrov, T. M. Borovskaya, Moscow Road Vehicle Institute; UDC 621.9.048:669.717]

[Abstract] The possibility of improving the antifriction characteristics of the AL25 and D16 aluminum alloys which satisfy Chapry's principle—the high wear resistance of a friction pair is ensured by the structural inhomogeneity of the "hard inclusions in a soft matrix" surface layer—by means of laser alloying from a coating is investigated. Three laser alloying procedures are used: applying a coat containing the alloying metals to the surface and laser treating individual tracks; applying a coat with alloying metal dicilicides to the surface and laser treating the whole surface; and applying a coat with the alloying metal dicilicides to the surface and forming individual laser tracks. The microhardness distribution in the alloying zone after saturation, the hardened AL25 sample mass behavior during the friction test, and the dry friction coefficient behavior of various hardened zones during the wear process are plotted and the microhardness of the hardened zones is examined under a Camebax electron microscope and Neophot-21 optical microscope. An analysis shows that the antifriction properties of the AL25 and D16 aluminum alloys may be indeed improved by laser alloying of the coated surface by developing the "hard inclusions in a soft matrix" heterogeneous structure in the surface layer; the necessary surface structure may be produced by varying the number of laser tracks as well as by manipulating the heterogeneity degree of the hardened zones. In friction pairs with steel 45, high antifriction properties are due to the metal dicilicides which form an inhomogeneous structure within each alloying zone. Figures 5; tables 1; references 3.

Sintering of Fused Mullite and Mullite-Corundum Composition Material Compacts

927D0119A Moscow OGNEUPORY in Russian No 9, Sep 91 pp 2-4

[Article by V. A. Ustichenko, N. V. Pitak, Ukrainian Scientific Research Institute of Refractory Materials; UDC 666.762.14.046.4]

[Abstract] The sintering of compacted blanks from fused mullite and mullite-corundum compositions which results in a decrease in the total particle surface, i.e., a decrease in the surface and total energy of the system, is investigated; powders produced by grinding and milling fused ingots with a mullite and mullite-corundum composition are used in the study. Fused mullite powders consist of 94 percent mullite grains and 6 percent glass while fused mullite-corundum powders consist of 48-53 percent mullite, 43-48 percent corundum, and 4 percent glass. The microstructure of fused mullite reduced in jet and vibratory mills is examined and the narrow fraction concentration of fused mullite ground in vibratory and jet-type mills, the dependence of the open and apparent porosity and volume shrinkage on the roasting temperature, and the dependence of the open and apparent porosity and volume shrinkage on the <20 μm fraction and fine component concentration are plotted. The experimental study demonstrates that the best sintering is attained in samples made from vibratory mill-ground powders which are characterized by a higher specific surface and a higher <10 μm grain concentration than the jet-type mill-ground powder. Refractories made from fuse mullite and roasted at a 1,750°C temperature have a high softening temperature under a 0.5 N/mm^2 load, generally higher than 1,750°C. Dense and strong refractory materials can be produced from a fused vibratory mill-ground mullite charge containing 60 percent or more of the <0.063 mm fraction while heat resistant refractories can be produced from a charge containing 30 percent of such fraction. Figures 7; tables 1; references 2.

Production Characteristics of Strong ZrO_2-Containing Ceramics

927D0119B Moscow OGNEUPORY in Russian No 9, Sep 91 pp 5-7

[Article by Ye. S. Lukin, N. A. Popova, N. I. Zdvizhkova, Yu. D. Garazhenko, V. A. Fomichenko, V. N. Donchenko, Moscow Chemical Engineering Institute and Donetsk Engineering Physics Institute; UDC 666.762.52-16]

[Abstract] The need for new structural materials with unusual mechanical and thermal properties prompted by technological and engineering development is recognized and the advantages of zirconium dioxide-based ceramic materials are discussed. Compaction parameters and sintering indicators of samples from ZrO_2 partially stabilized by 3 percent Y_2O_3 and by roasting at 1,650°C with a 10°C heating rate, exposure for one h, and cooling in the air are summarized. The mean ceramic density, crystal size, bending strength at various temperatures, microhardness, and HRC are measured. It is shown that production of such ceramics requires high-pressure hydrostats and gasostats with a 1,750-1,800°C heating temperature at a 1-2 GPa gas pressure. The need to improve and expand production of ZrO_2 powder with the necessary characteristics in the USSR is identified. Tables 2; references 16: 14 Russian, 2 Western.

Investigation of Effect of Heat Treatment on Zirconium-Alloyed Corundum Phase Composition and Properties

927D0119C Moscow OGNEUPORY in Russian No 9, Sep 91 pp 7-10

[Article by N. B. Zhekhanova, Urals All-Union Scientific Research Institute of Abrasives and Grinding; UDC 666.762.11+666.762.52].017:620.181.4]

[Abstract] The use of subeutectic Al_2O_3 alloys with ZrO_2—synthetic corundum—generally containing 23-25 percent (by mass) ZrO_2 in the abrasive industry for making grinding roughing wheels is discussed and the effect of heat treatment on the phase composition and physical and mechanical properties of zirconium-based synthetic corundum is investigated. To this end, grinding grains of the 38A6 synthetic corundum which differ in the melting and solidification conditions are examined. The phase composition is studied using a high-temperature X-ray phase analyzer in a DRON-2 unit with an URVT-2000 attachment in Cu*K* radiation; a Norton sample is used for comparison. The temperature dependence of the tetragonal ZrO_2 modification concentration on the heating and cooling temperature, the effect of heat treatment on the compressive strength and the tetragonal ZrO_2 modification concentration, the relationship between the grain strength and phase composition, and X-ray patterns of zirconium-based synthetic corundum are plotted and the corundum failure rate as a function of heat treatment is measured. An analysis reveals that heat treatment makes it possible to identify the instability of the material structure formed during its crystallization and cooling and the instability of its phase composition which is primarily due to the conditions of melt preparation for solidification. Figures 4; tables 3; references 7: 6 Russian, 1 Western.

Colloidal-Chemical and Rheological Properties of Aqueous ZrO_2 Suspensions and Their Interrelation With Casting and Product Properties

927D0119D Moscow OGNEUPORY in Russian No 9, Sep 91 pp 10-15

[Article by A. G. Karaulov, Ukrainian Scientific Research Institute of Refractories; UDC 666.762.52.001.4]

[Abstract] A study of the structural and mechanical characteristics of partially stabilized zirconium dioxide whose use is expected to facilitate production of heat

resistant products, such as crucibles, is reported; the possibility of eliminating the use of the initial monoclinic raw zirconium dioxide in order to improve the casting properties of suspensions is also examined. Pure grade TsRO-3 and TsRO-1 containing ZrO_2 and HfO_2 mixed with chalk are used to make the samples; the samples are then roasted, ground, and milled. After washing, the slip concentration is brought to 80 percent. The chemical composition of the stabilized zirconium dioxide after washing (in order to remove ground iron), the grain content of ZrO_2 stabilized with CaO from chalk, the casting properties of suspensions from stabilized zirconium dioxide, the effect of the monoclinic ZrO_2 addition to prestabilized zirconium dioxide on its structure and mechanical properties, the properties of suspensions, castings, and products from zirconium dioxide as a function of the monoclinic zirconium dioxide addition type and amount, the structural and mechanical properties of ZrO_2 suspensions at pH=2 and a 30 percent moisture content, and the properties of casting and products after roasting produced from zirconium dioxide suspensions with pH=3 and a 30 percent moisture content are summarized. Total rheological curves of TsRO-3 and TsRO-1 ZrO_2 suspensions stabilized with 12 percent and 8 percent CaO, the ZrO_2 suspension stability with and without monoclinic additions, the TsRO-1 casting wall thickness kinetics during casting, and the dependence of the TsRO-1 zirconium dioxide moisture content on the storage time are plotted. The study makes it possible to identify optimum casting parameters necessary to improve the production methods of zirconium dioxide items by the slip casting methods. Figures 7; tables 7; references 16: 15 Russian, 1 Western.

Friction Properties of Nitride Self-Propagating High-Temperature Synthesis Ceramics at Moderate Temperatures

927D0119E Moscow OGNEUPORY in Russian No 9, Sep 91 pp 15-17

[Article by I. P. Borovinskaya, V. E. Loryan, M. Yu. Blinov, V. D. Zozulya, Structural Macrokinetics Institute at the USSR Academy of Sciences; UDC 666.762.93.017:531.44]

[Abstract] The scarcity of published data on the friction properties of ceramic materials operating at a moderate temperature (>600°C) prompted a study of the tribotechnical properties of a sialon ceramic produced by the SVS method (high-temperature self-propagating synthesis) on the basis of silicon nitride with titanium carbide, silicon, boron nitride, and titanium nitride additions. High-temperature friction tests of samples heated to a 1,200°C temperature are conducted in a specially made friction testing machine which makes it possible to record the friction wear rate continuously. Wear tests are conducted by the contact method using a washer from steel 1Kh18N10T with a Al_2O_3-based ceramic coat sprayed onto it at a one m/s slip rate and a five N/mm^2 load. The dependence of the friction coefficient on the heating temperature, wear and friction coefficient digrams for various temperatures at a constant load, and the surface profile of the initial surface and friction surface of a Si_3N_4 sample with SiC and TiN are plotted. The microstructure of the sample friction surface and friction surface cross sections are examined. An analysis of the findings indicates that oxidation of the friction surface of SVS nitride ceramics improves the friction characteristics under the sliding friction conditions and that each friction pair is characterized by its own optimum operating temperature range. In general, the serviceability of nitride triboceramics is bounded by 800°C. The high surface finish degree of SVS friction ceramics at elevated temperatures is due to the amorphism of the antiscouring SiO_2 layers. The low friction coefficient of nitride SVS ceramics is attributed to the reduced hardness and certain fluidity of the antiscouring secondary structures forming during friction. Figures 5; references 8.

Mullite-Corundum Chamotte and Arkalyk and Berlin Clay-Based Products

927D0119F Moscow OGNEUPORY in Russian No 9, Sep 91 pp 23-26

[Article by R. S. Shulyak, V. V. Primachenko, L. N. Zolotukhina, V. N. Kungurtsev, V. A. Osipov, F. F. Ochertnyuk, Ukrainian Scientific Research Institute of Refractory Materials and Magnitogorsk Integrated Iron and Steel Works; UDC 666.762.11]

[Abstract] The technology of producing mullite-corundum chamotte and products on the basis of chamotte with Arkalyk and Berlin clays is examined and the raw material sources are comprehensively investigated. The chemical composition, percentage reduction in mass due to calcination, total fluxing oxide concentration, refractoriness, plasticity number, density, and baking of the Arkalyk and Berlin deposit clay and clay dust are summarized and the grain fracture distribution is measured. The microstructure of Arkalyk and Berlin clay is examined under an electron microscope and the dependence of shrinkage, water absorption, and open and apparent porosity on the roasting temperature is plotted. The properties of items with 80 percent Al_2O_3 are measured and compared to TU 14-8-140—75. The studies show that the Arkalyk and Berlin deposit clays can be used for making chamotte containing at least 85 percent Al_2O_3 (G-0 alumina) suitable for producing high-alumina refractory materials with the apparent density of freshly compacted samples reaching 2.88 g/cm^3. Figures 6; tables 4; references 2: 1 Russian, 1 Western.

New Heat Insulating Ultralight-Weight Corundum Material

927D0119G Moscow OGNEUPORY in Russian No 9, Sep 91 pp 26-27

[Article by N. V. Pisareva, Ye. A. Akselrod, S. I. Kulayenko, Ukrainian Scientific Research Institute of Refractory Materials; UDC 666.762.11-127]

[Abstract] The shortcomings of existing lightweight corundum materials with an apparent density of 1.1 g/cm^3 and a compressive strength at room temperature of 2.5 N/mm^2 are discussed and the development of a production method of ultralight-weight corundum products with an elevated mechanical strength is reported. The dependence of the mechanical properties of the new heat insulating material on its phase composition is examined and the effect of various mineral additives on mechanical properties is measured. The temperature dependence of the compressive strength of the new corundum material is plotted. An experimental batch produced at a pilot plant has a 97 percent Al_2O_3 concentration, an apparent density of 0.4 to 0.5 g/cm^3, a compressive strength at room temperature of 2.0 to 4.5 N/mm^2, a thermal conductivity a 350°C of 0.37 and at 600°C—of 0.45 W/(m ^{x} K), and a softening onset temperature at a 0.2 N/mm^2 load of 1,260-1,300°C; it also has no additional shrinkage at 1,550°C. The experimental batch is used in the lining of electric furnaces and reveals no visible changes after two years of operation. Figures 1.

Corundum-Graphite Monoblock Stoppers for Continuous Casting Machines

927D0119H Moscow OGNEUPORY in Russian No 9, Sep 91 pp 31-34

[Article by L. M. Akselrod, All-Union Institute of Refractory Materials; UDC 666.762.11+666.762.8]: 621.746.329.047]

[Abstract] The corundum-graphite monoblocks stoppers manufactured at a number of refractory plants and used in the intermediate ladles of continuous casting machines (MNLZ) are reviewed; both conical and spherical head section designs are considered. The methods of monoblock stopper fastening by studs or threaded joints are analyzed and the relative advantages of delivering an inert gas to the metal thought the monoblock stopper are discussed. The chemical composition, open porosity, and gas permeability characteristics of monoblock stoppers and gas permeable fittings made in the USSR and by the Vesivius Company (U.S.), OAMAG (Austria and Germany), and Sirma (Italy) are summarized and compared and the most frequent characteristic deviations from specifications which worsen the quality of refractory products and their likely consequences are examined. It is shown that the operating reliability of monoblock stoppers can be improved, their consumption may be decreased, and the efficiency of continuous steel casting may be increased by giving more attention to their production and by using them more skillfully. Figures 5; tables 2; references 12: 2 Russian, 10 Western.

Fracture of Reinforced Concrete Beams With Mixed Reinforcement Under Dynamic Loads

927D0121A Moscow BETON I ZHELEZOBETON in Russian No 11 (440), Nov 91 pp 4-5

[Article by N. N. Popov, M. Charyyev; UDC 624.072.012.35.42]

[Abstract] The advantages of using combined reinforcement methods by mixing prestressed reinforcement rods with soft nonstressed rods in order to lower the consumption of steel and protect the structure from sudden brittle failure are discussed and freely supported and constrained mixed-reinforced concrete beams are investigated under dynamic loads. The dependence of the bending moment on curvature is plotted on the basis of a statistical analysis of the test data and the reinforcement configuration is cited. The results show that the use of the combined reinforcement arrangement is necessary for ensuring that after the rupture of the prestressed high-strength reinforcement bars, the structure retains sufficient load-bearing ability for absorbing static load forces and that this may be attained by increasing the proportion of soft reinforcement bars to 50 percent and by designing statically indeterminable constructions. The use of combined reinforcement is especially efficient in the case where the dynamic loads are applied during a time span shorter than the total structure time to fracture. Figures 2; tables 1; references 2.

Increasing Concrete Efficiency by Adding Modified Lignosulfonates

927D0121B Moscow BETON I ZHELEZOBETON in Russian No 11 (440), Nov 91 pp 10-11

[Article by Yu. M. Bazhenov, G. V. Anosova, G. I. Yevorenko; UDC 666.572.16]

[Abstract] The addition of modified lignosulfonate-based hydrophobe plasticizers to concrete in order to improve its physical and mechanical properties is discussed and a study of the physical and mechanical properties of concrete mix and concrete with an ST admixture pursuant to "Recommendations on evaluating the efficacy of admixtures to concrete" is reported. Portland cement 400, hard rock gravel from the Vyazma quarry, granite gravel, sand, and tap water are used as the ingredients. The chemical composition of the cement clinker and its mineralogical content and the normal viscosity, setting time, activity, and milling dispersity of two brands of cement are summarized. An analysis of the findings indicates that the use of the ST admixture within an optimum range makes it possible to increase the concrete mix mobility from 2-4 to 16-18 cm without lowering the concrete strength or to increase the strength of concrete made from mix with a varying mobility at the same cement outlays by at least 35-50 percent as well as decrease the cement consumption by at least 10 percent per 1 m^3 of concrete using equal-flowability mix. The ST admixture does not contribute to the reinforcement corrosion and may be used for making prefabricated constructions. An addition, the use of the ST admixture shortens the vibration tamping time. The ST costs 42-45 rubles per ton and its economic impact is close to 2,000 rubles per ton. Tables 3.

Fast-Hardening Composite Gypsum Binders, Concretes, and Products

927D0121C Moscow BETON I ZHELEZOBETON in Russian No 11 (440), Nov 91 pp 17-18

[Article by V. F. Korovyakov, A. V. Ferronskaya, L. D. Chumakov, S. V. Ivanov; UDC 691.54.001.1]

[Abstract] Methods of decreasing the consumption of concrete for low grade (≤V15) products by using more efficient binders are discussed and the properties and production cost of fast-hardening composite gypsum-based binders as well as concrete and concrete products are investigated. The study is aimed at developing binders with a less than 15 percent clinker concentration which make it possible to increase the concrete strength by 1.3-1.5 times and increase the water and cold resistance; developing durable concretes and items on their basis which do not call for heat treatment and require lower outlays of energy, metal, and labor; and developing automated pilot production lines for making composite gypsum binders and products on its basis. Lab studies of such products made at the All-Union Scientific Production Association of Wall and Binding Materials make it possible to assert that the product is water resistant and its strength is higher than that of the original gypsum binder by 1.3-1.5 times while its clinker concentration does not exceed 15 percent. The use of the gypsum binder makes it possible to save 175-195 t of portland cement per 1,000 m^3 of concrete, i.e., increase the portland cement yield by five- to sixfold and decrease the electric power outlays by two- to threefold. References 3.

Polyelectrolytic Complex-Based Superplasticizer

927D0121D Moscow BETON I ZHELEZOBETON in Russian No 11(440), Nov 91 pp 18-20

[Article by L. I. Simonenko, V. I. Stambulko; UDC 666.572]

[Abstract] The use of chemical additives for increasing the corrosion resistance and service life of concrete and grouting mortar is discussed and the efficacy of using a superplasticizer, whose polyfunctional nature and chemical interaction with the portland cement hydration products make it especially cold and salt resistant, for this purpose is considered. To this end, the behavior of concrete with polyelectrolytic complex-based superplasticizers is examined in a corrosive environment which simulates the operating conditions of the oil and gas wells in the far north. The methods underlying principles for producing polyelectrolytic complexes which are characterized by a high plastic activity due to the concentration of active functional groups in its molecules are developed. The use of this admixture increases the concrete strength and impregnability, lowers the water/cement ratio, increases the microporosity, and binds calcium hydroxide. In addition, the use of the superplasticizer lowers the water consumption by 10-30 percent, increases the concrete and grouting mortar strength considerably, doubles the cold resistance, and quintuples the salt resistance. Tables 3.

Guniting Technology of Radioabsorbing Concrete

927D0121E Moscow BETON I ZHELEZOBETON in Russian No 11(440), Nov 91 pp 20-21

[Article by O.V. Belousov, N.T. Mambetaliyev; UDC 666.033.14:621.396.669]

[Abstract] The ecological importance of materials capable of screening and absorbing electromagnetic radiation prompted the development of a Gunite spaying technology of placing electromagnetic radiation absorbing concrete and forming concrete products with its help. A schematic diagram of the method's implementation is cited. The concrete mix consists of graphite, a hardening agent, a pore-forming agent, and a carbon-containing additives—inexpensive and easily available materials. A sodium silicate solution with a density of 1.44 g/cm^3 and a 2.7 silicate modulus is used as the binder. The radiophysical properties of the radioabsorbing concrete are examined using a specially developed technique. The concrete has a 0.05-0.9 percent reflectance. The resulting radioabsorbing concrete is characterized by a high compressive strength and elevated fire resistance and meets the specifications of the SNiP construction rules and regulations. Figures 1.

Interrelation of Biaxially Compressed Concrete Strength Diagram and σ-ε Characteristics Under Uniaxial Compression and Tension

927D0121F Moscow BETON I ZHELEZOBETON in Russian No 11 (440), Nov 91 pp 24-26

[Article by V. N. Baykov; UDC 69.059.22]

[Abstract] The relationship between the strength diagrams of biaxially compressed concrete and its σ-ε characteristics under uniaxial compression and tension is discussed and concrete strength diagrams of concrete are plotted under uniaxial compression and uniaxial tension for a prism-shaped sample. An attempt is made to predict the concrete sample behavior under biaxial loads on the basis of data obtained in uniaxial tests. The strain diagram of biaxially loaded prismatic concrete samples is also plotted and analyzed. A comparison of the strength diagrams reveals that the material is strained simultaneously in the longitudinal and transverse direction and the strain is interrelated. The internal stresses developing in the biaxially strained samples in oblique directions significantly affect the stressed state of concrete. The findings indicate that biaxial compression of concrete increases its axial strength and confirm the efficacy of biaxial concrete compression in construction applications. The effect of the higher concrete strength in a biaxially strained state may be used in designing reinforced concrete structures as an additional reserve for increasing their load bearing ability. Figures 3; references 7: 6 Russian, 1 Western.

Moisture-Induced Strain in Concrete With Admixtures Under Freezing and Thawing Cycles

927D0121G Moscow BETON I ZHELEZOBETON in Russian No 11 (440), Nov 91 pp 29-30

[Article by V. O. Almazov, O. V. Starchenko; UDC 624.072.3]

[Abstract] The considerable moisture-induced expansion strain developing in concrete under freezing-thawing cycles and its effect on the operation of elements under extended loading are investigated. To this end, prism- and slab-shaped samples made from concrete at a 1:1.2:2.2 cement/sand/gravel ratio and a 0.32 water/cement ratio with a complex additive consisting of 0.7 percent S-3 and 0.15 percent GKZh-94 are tested. The samples' side surfaces are not moisture proofed. The moisture content before and after the experiments, which include 30 freezing-thawing cycles followed by an exposure to a positive temperature for 120 days and 70 more freezing-thawing cycles, is measured. A chart of moisture-induced straining during the freezing-thawing cycles is plotted. Formulae are derived for determining the moisture-induced concrete strain as a function of the scaling factor. An analysis of the results shows that a change in the scaling factor changes the moisture-induced strain in concrete modified with additives. The use of the proposed formulae makes it possible to predict the moisture-induced strain allowing for the scaling factor and the initial moisture content. A comparison of analytical and experimental data confirms that the theoretical results are consistent with the results of experimental studies. Figures 1; tables 3; references 4.

Straining Processes During Diamond Powder Sintering Under High Pressure Conditions. Report 2

927D0123A Kiev SVERKHTVERDYYE MATERIALY in Russian No 4 (73), Sep-Oct 91 pp 3-6

[Article by V.F. Britun, G.S. Oleynik, N.P. Semenenko, Institute of Materials Science Problems at the Ukrainian Academy of Sciences, Kiev; UDC 666.233]

[Abstract] Continued from SVERKHTVERDYYE MATERIALY No 3, 1991. The diamond straining mechanisms occurring at 1,800-2,500°C temperatures, which are characterized in that they occur in the already strained grains, are investigated. The strain structure develops as a secondary structure on the basis of the substructure forming during the pretreatment stage indicating this the case under study is not "pure" high-temperature diamond straining. This fact is used to explain a number of crystallographic peculiarities inherited from the high-temperature strain substructures typical of low-temperature straining conditions. The studies are performed by the transmission electron microscopy methods. The results suggest that the plastic flow observed within a broad temperature range develops without an abrupt change in the straining mechanisms, making it possible to speculate that the brittle plastic transition in diamond is rather blurred. Figures 4; references 2.

Controlling Wettability and Contact Interaction of Metallic Melts With Graphite and Diamond Surface

927D0123B Kiev SVERKHTVERDYYE MATERIALY in Russian No 4 (73), Sep-Oct 91 pp 7-12

[Article by V. M. Perevertaylo, Superhard Materials Institute at the Ukrainian Academy of Sciences, Kiev; UDC 541.183:669.65]

[Abstract] The results of an investigation of the adhesion phenomena and wettability in graphite (diamond)/metallic melt contact systems, which make it possible to establish the behavior patterns of the capillary characteristics of the interface at various controlled degrees of the contact system deviation from the thermodynamic equilibrium state and to draw a number of conclusions about the physical and chemical patterns of capillarity and the character of motive forces of the process occurring in the solid/liquid contact systems and methods of manipulating their wettability, are analyzed and summarized. It is noted that the capillarity patterns in the melt/carbonaceous material system may be extended to other types of systems where a metallic melt is in contact with the solid phase of various physical and chemical origins, e.g., carbides, nitrides, oxides, etc; in this case the contact processes on the solid/liquid interface should be analyzed allowing for the liquid's interaction with all component elements of the solid surface. Figures 5; references 10.

Interference Effect of Two Types of Paramagnetic Centers Penetrating Synthetic Diamond Crystals

927D0123C Kiev SVERKHTVERDYYE MATERIALY in Russian No 4 (73), Sep-Oct 91 pp 16-19

[Article by L. A. Shulman, Superhard Materials Institute at the Ukrainian Academy of Sciences, Kiev; UDC 539.291:621.921.34]

[Abstract] The principle of the least free energy of the system is used to examine the cross-interference of the Ni and N impurity centers which are simultaneously penetrating synthetic diamond crystals. The correlation of Ni and N concentrations is examined experimentally at a 77K temperature; it is noted that the cross-interference of the above impurities penetrating a matrix also occurs in other crystals; a similar phenomenon is observed during the penetration of rare earth ion impurities into crystals of mixed garnets. The interaction energy is found in two extreme cases of impurity concentrations. An analysis of the findings indicates that the system displays a tendency to a predominant substitution of lattice sires with nitrogen atoms when the Ni center concentration is low and vice versa, i.e., to a substantial increase in the Ni center concentration with

a decrease in the N concentration; moreover, the least energy principle is realized in both cases. Figures 2; tables 1; references 12: 10 Russian, 2 Western.

Study of Ti-B-C System Phase Equilibria and Properties of Resulting Samples

927D0123D Kiev SVERKHTVERDYYE MATERIALY in Russian No 4(73), Sep-Oct 91 pp 19-25

[Article by Yu. N. Vilk, Central Scientific Research Institute of Materials, Leningrad; UDC 669.295;781-194.017:620.179.15]

[Abstract] Studies of the constitution diagrams of Ti-B-C systems and the behavior of these systems at different temperatures performed by various authors are reported; Ti-B-C alloys in various phase fields of the ternary system are investigated; the alloys are produced by melting in an arc furnace. The chemical composition of the powders used as the source materials is summarized and an isothermal cross section of the Ti-B-C system is plotted at a 1,800K temperature. The properties of alloys smelted from titanium carbide, Ti, and boron carbide powder are examined by microstructural, radiographic, and X-ray spectral analyses; the phase composition of the alloys is identified and the element distribution is determined. The abrasive and strength properties of these materials' grains are investigated. It is shown that grains of alloys in the TiC-TiB_2 and TiC-TiB fields are distinguished by higher strength and abrasive ability than those of the grains of conventional abrasive materials and exceed the properties of synthetic corundum and silicon carbide in this respect; they approach boron carbide in abrasive properties. Figures 2; tables 2; references 16: 12 Russian, 2 Western.

Protective Si-N-C Ceramic Coats on Quartz Glass

927D0123E Kiev SVERKHTVERDYYE MATERIALY in Russian No 4 (73), Sep-Oct 91 pp 29-32

[Article by P. I. Andriyenko, A. G. Varlamov, Yu. M. Grigoryev, Structural Macrokinetics Institute at the USSR Academy of Sciences, Chernogolovka, Moscow oblast; UDC 549.527:546.281]

[Abstract] The effect of the Si-N-C coating's chemical composition and synthesis conditions on the strength of the cylindrical quartz base/protective coat pair is investigated; the coats are deposited by the CVD method onto a heated quartz substrate with the help of electric thermography; the deposition method is based on controlled heating of the samples in a medium of gaseous reagents. The condensed film is produced by pyrolysis of the gaseous mixture of tetramethylsilane (TMS), hydrazine (G), and hydrogen under isothermal conditions at the substrate surface temperature of 1,000-1,300°C for 2-840 s. The design of the deposition unit is described. An analysis shows that coats containing five to 12 percent C by mass produced at a 1,080°C temperature are the most compatible with the quartz base; they have the lowest tendency to cracking and the lowest ultimate bending strength. The results demonstrate that the strength properties of Si-N-C coats on cylindrical quartz samples are not a unique function of their chemical composition but are related to the synthesis conditions which affect the coat's cracking. Figures 3; references 7: 3 Russian, 4 Western.

Compaction Under Electric Current Sintering of Noncompacted Metallic Powder Particles

927D0114A Kiev POROSHKOVAYA METALLURGIYA in Russian No 1 (349), Jan 92 pp 23-27

[Article by G. L. Burenkov, A. I. Raychenko, A. M. Surayeva, Institute of Materials Science Problems at the Ukrainian Academy of Sciences; UDC 621.762]

[Abstract] The behavior of the powder sample density during the electric current sintering is discussed and an attempt to reveal the effect of electric factors on the sintering dynamics of spherical powders during their compaction by electric current is reported. The sintering process is tentatively divided into three phases: initial contact skeleton formation, predominant destruction of some of its segments, and formation of contact necks with their subsequent improvement and increase in the cross section area. Atomized powders from the BrOF-10-1 alloy with a 0.1-0.3, 0.4-0.63, and 0.8-1.0 mm grain size variation are sintered by alternating current in a quartz mold and the samples' dynamic and static density is measured; the effect of the external mechanical pressure on the shrinkage kinetics of spherical bronze particles, the dependence of the sample porosity on the electric current sintering duration, and the dependence of the sample porosity on the particle size are examined and plotted. The time dependence of the spherical particle compaction during sintering displays three phases: at the initial and final stages, compaction occurs at a lower rate than at the mid-phase. An initial loosening followed by compaction is observed during a continuous recording of linear changes. It is demonstrated that an increase in the current density enhances shrinkage and shortens the loosening period duration while an increase in the mechanical pressure is accompanied by a decrease in the compaction rate. Figures 3; tables 1; references 8.

Structure and Properties of Nickel-Chromium Diboride Alloys

927D0114B Kiev POROSHKOVAYA METALLURGIYA in Russian No 1 (349), Jan 92 pp 32-37

[Article by V. N. Yanenskiy, Yu. A. Gusliyenko, I. M. Fedorchenko, Institute of Materials Science Problems at the Ukrainian Academy of Sciences; UDC 621.357.7:669.248.7]

[Abstract] Ways of improving the properties of composite nickel-based electrolytic coats with chromium diboride inclusions by heat treatment are discussed and the structure, hardness, and wear resistance of Ni-Cr-B system alloys with 0-2.8 percent CrB_2 are investigated. Constitution diagrams of the corresponding binary systems, isothermal cross sections of the B-Cr-Ni system, and its liquidus surface are plotted, and the polythermal cross section of this system is plotted along the Ni-CrB_2 line. It is shown that as the chromium diboride concentration increases in the initial sinter after fusion in a vacuum, alloys with a structure of the Cr solid solution in Ni surrounded by a boride frame with various ratios of structural components and binary and ternary eutectics with surplus solid phases in the eutectic matrix are formed. As the cooling rate of heat treatment increases during the alloy solidification, eutectic colonies and surplus solid phases are fragmented, and the eutectic dispersivity increases. An increase in the CrB^2 concentration in the composition after fusion increases the alloy hardness and wear resistance. In order to ensure the maximum wear resistance under the abrasive friction conditions, the CrB_2 content in nickel-based alloys must be maintained within 20 percent while the solidifying alloy should be cooled at the highest possible rate. Figures 4; tables 1; references 8.

Comparing Properties of Porous Materials From Various Metallic Fibers and Powders

927D0114C Kiev POROSHKOVAYA METALLURGIYA in Russian No 1 (349), Jan 92 pp 45-48

[Article by O. V. Kirichenko, A. A. Dubikovskaya, V. G. Lapshin, Institute of Materials Science Problems at the Ukrainian Academy of Sciences; UDC 621.762.5:669:621:763:620.178]

[Abstract] Porous materials sintered from drawn metallic fibers are compared to those made from powders; to this end, the principal structural characteristics and hydrodynamic and physical and mechanical properties of porous materials from powder fibers are compared to the like characteristics of comparable porous materials from drawn fibers and powder. The permeability of porous materials made from powder fibers with a 5-28 μm diameter is measured according to GOST 25283—82, and the pore dimensions are measured according to GOST 26849—86 and by the mercury pore measurement method. The bulk pore content in powder and drawn fiber materials, the dependence of the pore irregularity parameter of fiber and powder materials on their porosity, and the dependence of toughness, ultimate tensile strength, shearing and bending strength, and elongation of materials sintered from powder and fibers are plotted. The permeability coefficient of porous materials as a function of their ultimate tensile strength is calculated. The findings show that given an identical porosity and the same fiber diameter, powder fiber materials have a smaller pore size than drawn fiber materials but are characterized by lower permeability and mechanical strength indices. Powder fiber materials have a more uniform structure at an equal porosity while materials from powder fibers occupy an intermediate position between porous materials from drawn fibers and powders with respect to their permeability coefficient and permeability/pore diameter ratio. Figures 3; tables 1; references 9.

Effect of Annealing on Structure and Properties of Hot-Compacted Boron Carbide

927D0114E Kiev POROSHKOVAYA METALLURGIYA in Russian No 1 (349), Jan 92 pp 69-72

[Article by A. A. Korneyev, I. T. Ostapenko, M. A. Dolzhek, A. G. Mironova, N. D. Rybalchenko, I. A. Lyashenko, V. P. Podtykan, Kharkov Engineering Physics Institute; UDC 546.27'26:539.531:539.56]

[Abstract] The effect of the structure and composition of hot-compacted B_4C on its physical and mechanical properties which, in turn, are the principal factor affecting the behavior of products under thermal and force loading are analyzed, and the processes of accumulative recrystallization of hot-compacted boron carbide grains with subsequent annealing in a vacuum are examined; in addition, the physical and mechanical properties, e.g., microhardness and fracture toughness, of the grains are determined. Test samples are cut from hot-compacted blanks by the electrospark method and are annealed in a vacuum at 1.33 Pa within an 1,873-2,523K temperature range. The microstructure is examined under optical and electron microscopes. The microhardness of heat treated samples is measured in a PMT-3 hardness gauge under a 1 N load. The dependence of the microhardness and fracture toughness of B_4C on the annealing temperature and the dependence of the B_4C grain fracture toughness on the grain size within a 1-30 μm range are plotted. An analysis demonstrates that the microhardness of hot-compacted boron carbide linearly decreases from 43 to 35 GPa while the fracture toughness peaks at a 2,373K temperature. This behavior is attributed to a change in the material structure during annealing. At temperatures above 2,373K, the accumulative recrystallization processes are the most active, and the structure is characterized by a grain size irregularity and the presence of a large number of growth twins, while pores coalesce and grain boundary defects form. Figures 4; references 8: 6 Russian, 2 Western.

Surface Layer Temperature and Structural Distortions During Polycrystalline Tungsten Grinding

927D0114F Kiev POROSHKOVAYA METALLURGIYA in Russian No 1 (349), Jan 92 pp 72-77

[Article by A. A. Adamovskiy, D. V. Lotsko, Yu. V. Milman, T. V. Chernenko, Institute of Materials Science Problems at the Ukrainian Academy of Sciences; UDC 621.7.016.019:620.191]

[Abstract] The effect of the near-surface temperature on the quality of ground metal surface whereby nearly 97-98 percent of energy is converted to heat is discussed, and the effect of the surface layer temperature of polycrystalline tungsten in the cutting zone on the structural distortions and the character of fracture during grinding is investigated in order to construct the fracture mechanism. Polycrystalline arc-smelted pure tungsten process-annealed for one hour at 1,400°C is ground without a lubricant-coolant fluid in a 3G71M machine. Temperature curves recorded by a microthermocouple during the grinding of polycrystalline tungsten by various types of grinding wheels to a 0.01 mm depth are cited, and the grinding wheel characteristics are summarized. The maximum cutting zone temperature during the tungsten grinding by various types of grinding wheels and the X-ray diffraction line broadening of W samples ground by these wheels are plotted. The surface microstructure is examined under a scanning electron microscope. Most of the grinding conditions lead to the development of a 0.02 s thermal pulse in the contact zone with a maximum temperature within the tungsten fracture range by the delamination mechanism. After grinding, an X-ray diffraction line broadening anisotropy is observed; it is similar to that of FCC metals after warm rolling. The broadening increases with temperature to 500-550°C, then stabilizes to 950°C, attesting to an equilibrium between the straining and relief processes. Figures 4; tables 1; references 13: 12 Russian, 1 Western.

Cutting Properties of Shock Wave-Sintered BN_{sph} Polycrystals

927D0114G Kiev POROSHKOVAYA METALLURGIYA in Russian No 1 (349), Jan 92 pp 81-87

[Article by V. I. Kovtun, V. P. Alekseyevskiy, A. V. Bochko, V. G. Peleshchuk, G. G. Karyuk, V. I. Trefilov, Institute of Materials Science Problems at the Ukrainian Academy of Sciences; UDC 548.33]

[Abstract] Unique properties of cutting blade tools from diamond and dense boron nitride modifications and the shortage of data on the operating (abrasive and cutting) properties of hard alloy tips sintered in shock waves prompted an examination of BN_{sph} polycrystals. Large polycrystals are produced by complete or partial sintering of a BN_{sph} powder without a binder. The BN_{sph} polycrystal hardness after shock wave compaction and treatment at seven and eight GPa and at 2,023 and 2,273K is studied, and the BN_{sph} polycrystal porosity, phase composition, dislocation density, and second-kind microdistortions are summarized. The polycrystal surface is examined before and after grinding, the cutting tip wear as a function of time is plotted, the cutter wear after turning for 1.5 min is analyzed, and the diffusive transport in the cutting tips is investigated. The study demonstrates that the wear of shock wave-sintered polycrystals is 20 percent lower, and the wear of polycrystals after the thermobaric treatment is 30 percent lower than that of elbor borazon P. The difference is attributed to the substructure characteristics and the diffusion process intensity on contact surfaces. The diffusion phenomena developing during the cutting of steel KhVG by BN_{sph} sintered tips have a negative effect on both products; this

fact should be taken into consideration in selecting the material for machining. Figures 5; tables 1; references 11: 10 Russian, 1 Western.

Experience of Commercial Production of Electrolytic Powders

927D0114H Kiev POROSHKOVAYA METALLURGIYA in Russian No 1 (349), Jan 92 pp 92-97

[Article by O. A. Potapov, I. B. Murashova, S. L. Korkin, A. V. Pomosov, A. T. Krestyaninov, Urals Polytechnic Institute; UDC 621.762]

[Abstract] The rising demand for powders characterized by an elevated bulk density and fluidity prompted a study of the methods of producing filled copper powders by the galvanodynamic method that ensures a high electrolyzer yield. The galvanodynamic electrolysis parameters, i.e, the initial current density, the rate of current increase, and the cathode overvoltage, are measured in lab tests, and the polarization curves of copper discharge on the commercial electrolyzer and copper powder fraction distribution during the powder treatment are plotted. The experimental conditions calculated by statistical processing of the results on an Iskra-1256 computer are described. The bulk density dynamics of the PMS-V powder after dry treatment are plotted; after grinding, the powder density falls within a 2.4-2.7 g/cm^3 range. It is shown that an increase in the $CuSO_4$ copper sulfate in the electrolyte from 0.25 to 0.32 mol/l makes it possible to double the initial current and slightly increase the current scan rate and the discharging ion concentration, thus increasing the electrolyzer yield. The powder particle size distribution maximum falls at the 45 μm fraction while the 63-100 μm fraction concentration decreases from 32 to 20 percent after the post-electrolysis treatment. Figures 3; tables 3; references 7: 6 Russian, 1 Western.

Permanent Anisotropic Ferromagnetic Powder Magnets With Organic Composite Coating

927D0114I Kiev POROSHKOVAYA METALLURGIYA in Russian No 1 (349), Jan 92 pp 101-103

[Article by V. V. Nepomnyashchiy, Institute of Materials Science Problems at the Ukrainian Academy of Sciences; UDC 621.752.4;538.221;669.517.255]

[Abstract] The difficulty of permanent magnet production from iron-based powders by compaction is discussed and the properties of permanent magnets compacted from powder particles with a shape anisotropy in a strong magnetic field are investigated. Magnet powders from pure iron and an iron-cobalt alloy are made in a double-layer electrolytic bath and exposed to reduction annealing. A special unit induces an up to 1,600 kA/m magnetic field in the mold located inside a magnetizing device. A schematic diagram of the magnetic field compaction mold is presented, and the dependence of the parameter α that characterizes the particle orientability on the magnetic field strength during the iron-cobalt powder magnet molding is plotted. When a 1,600 kA/m magnetic field is used, α increases to 0.8 which is quite acceptable for the above powders. The dependence of the properties of anisotropic and isotropic magnetic materials produced by warm compaction on the material composition is summarized, and the microstructure of Fe-Co alloy particles with an organic composite coat is examined. The conclusion is drawn that the method of warm compaction with magnetic field application makes it possible to produce permanent magnets whose magnetic properties are comparable to those of commercial cast YuNDK-15 and -18 alloys. Figures 3; tables 1; references 5.

Adding Copper to Powder Materials by Electrolytic Cladding Method

927D0114J Kiev POROSHKOVAYA METALLURGIYA in Russian No 1 (349), Jan 92 pp 103-105

[Article by L. M. Kurvyakova, Yu. N. Zhirkova, O. G. Taranov, Novomoskovsk Branch of the Moscow Chemical Engineering Institute and Tulachermet Scientific Production Association; UDC 621.762:669.38]

[Abstract] The shortcomings of the method of improving the YuNKT powder compactability by adding up to 4 percent (by mass) copper powder to the charge are discussed and the conditions for electrochemical copper-cladding of the YuNKT magnetic powder that ensure a uniform copper distribution both within each grain and throughout the burden are examined; in addition, the properties of copper-clad powders are investigated. Electrolytes generally recommended for copper cladding in electrodeposition are various copper-cladding electrolyte compositions, electrolysis conditions, and deposit properties are summarized and the dependence of the anode and cathode copper current efficiency on the current density, given a 60 g/dm^2 powder charge, is plotted. The oxygen concentration in the YuNKT powder before and after copper-cladding is measured and the copper-clad particle structure is examined. The following electrolyte composition is recommended: 80 g/l $CuSO_4 \times 5H_2O$ + 320 g/l $K_4P_2O_7$ + 5 g/l KOH + 20 g/l trilon B. The optimum (from the viewpoint of the coat quality and operating stability) anode and cathode current density ratio is 1:3. It is suggested that copper-clad powders be treated in a 0.02 percent soap solution and then dried in a vacuum. Compacted copper-clad YuNKT products have a higher density than those of the initial mixture, both before and after sintering, and are characterized by a higher sintering temperature. Figures 2; tables 2; references 2.

Improving Quality of Sections From Conticast Bearing Steel and Increasing Bearing Service Life

927D0115C Moscow STAL in Russian No 1, Jan 92 pp 29-31

[Article by V. I. Listopad, I. K. Nikolayev, O. L. Klimenkova, Central Scientific Research Institute of Ferrous

Metallurgy, Hammer and Sickle Metallurgical Works, and State Bearing Plant No 1; UDC 669.18-147:621.771.22]

[Abstract] The issue of producing sections from continuously cast bearing steel ShKh15-U and ShKh15SG-U and monitoring the axial segregation is addressed, and experimental tests of the quality of conticast bearing steel developed at the Donetsk Metallurgical Works are described. The effect of the oxygen concentration in steel on the actual service life of bearings (rather than samples) is studied. To this end, cold-finished steel ShKh15-U with a 0.0052 percent oxygen concentration is tested; the results do not show a direct correlation of the oxygen concentration in the metal and the oxygen-containing nonmetallic inclusion concentration according to GOST 801—78. The quality of cold-finished steel SkKh15-U made by the SUOLZ and conventional electroslag refining method and the quality of 14.288 mm dia. bearing balls from steel ShKh15-U produced by the SUOLZ process (from continuously cast ingots) is evaluated by the GPZ-1 technique, and the life of pilot bearings and the number of inner raceway loading cycles are plotted. The relative advantages of the SUOLZ method vs. the electroslag refining (EShP) are assessed. Bench tests show that the longevity of pilot bearings with balls made from conticast metal smelted by the SUOLZ method is higher than that of commercial earnings made from the electroslag refined metal. Figures 1; tables 2; references 1.

Secondary Aluminum Smelting Waste Utilization in Tube Steel-Making

927D0115G Moscow STAL in Russian No 1, Jan 92 p 86

[Article by N. G. Yaraliyev, R. K. Kuliyev, B. I. Podzharskiy, Azeri Tube Rolling Mill; UDC 669.054.8.004.02]

[Abstract] Experimental design work on mastering resource-saving method of utilizing the byproducts and waste from secondary aluminum production for making carbon steel, particularly for deoxidizing carbon tube steels for use in the petroleum industry and for reducing the ferrosilicon consumption by 45 percent, is reported. To this end, the aluminum waste from the Sumgait aluminum smelter containing 50-80 percent Al_2O_3, 8-25 percent Al_{met}, 10 percent SiO_2, and 5 percent Cu+Zn is used. The deoxidation procedure is outlined; a metallographic analysis of the blooms shows that the quality of the metal remains unaffected. The anticipated annual savings exceed 128,000 rubles.

Experience of Utilizing Secondary Resources at Magnitogorsk Cold-Finished Bar Plant

927D0115H Moscow STAL in Russian No 1, Jan 92 pp 86-88

[Article by V. V. Krivoshchapov, Ye. A. Pudov, Magnitogorsk Cold-Finished Bar Plant; UDC 669.054.8]

[Abstract] The urgency of resource-saving technologies and secondary resource utilization in rolled and drawn stock production is emphasized and the experience accumulated at the Magnitogorsk Cold-Finished Bar Plant (MKZ) in utilizing process waste of rolled and drawn stock production is outlined. In particular, the use of shavings and other scrap from the production of cold-finished steel bars and mounting hardware and methods of collecting and sorting out the shavings and nut metal scrap for various brands of steel strictly according to their specified chemical composition is summarized. Secondary resource application is also illustrated by the use of metal band scrap for making staples and other fasteners as well as the use of the waste water from the Uzbek Integrated Refractory and High-Temperature Alloy Works in Chirchik, primarily the saltpeter, for wire patenting. The economic impact from the saltpeter recovery is estimated at more than 40,000 rubles.

Pyrothermal Treatment of Welded Joints

927D0118A Moscow METALLOVEDENIYE in Russian No 10, Oct 91 pp 4-5

[Article by S. V. Serikov, R. Sh. Idiyatullin (deceased), S. N. Myakushkin, V. V. Yaufman, UralNITI and Kazan Chemical Engineering Institute; UDC 662.1:671.774.21:621.643]

[Abstract] Various methods used to lower the residual welding stress are discussed and the possibility of using heat treatment of welded pipe joints for this purpose, whereby the treated surface is heated due to the combustion of a pyrotechnic material, is assessed; to this end, slabs of the TI-5 pyrotechnic thermite material are attached along the pipe perimeter on the welded joint surface and ignited while thermocouples connected to recording equipment are placed on the inside surface of the slabs and the residual stress structure and distribution in the joints are measured with the help of bonded strain gauges. Thermograms of the welded joint are plotted during the combustion of various thermite layer configurations. A metallographic analysis of the welded joint as well as an evaluation of the residual stress level before and after the pyrothermal treatment make it possible to recommend this procedure in place of traditional heat treatment methods. It contrast to the highly efficient detonation treatment, a much broader range of temperature gradients on the treated part surface may be realized by using the pyrothermal method. Figures 5; references 5.

Corrosion Resistance of Electrical Sheet Steel After Aluminizing

927D0118I Moscow METALLOVEDENIYE in Russian No 10, Oct 91 p 43

[Article by S. G. Babich, A. A. Zyabrev, G. V. Skibina, V. D. Kiselev, Physical Chemistry Institute imeni L. Ya. Karpov at the Moscow State Engineering University

imeni N. E. Bauman; UDC 620.194.8:669.14.018.298.3:621.793.6]

[Abstract] Soft magnetic electrical sheet steel 20895 used for making instrument relays is aluminized by the circulation method based on the principle of diffusing element transport within a closed working volume during the systematic reduction of the transfer agent gas due to reversible chemical reactions. The corrosion resistance of steel 20895 is examined both before and after aluminizing with the help of a P5827M potentiostat and PI-50 device during tests in a 3 percent HCl solution at 20°C. Polarization curves of steel 20895 before and after aluminizing are plotted. An analysis demonstrates that aluminizing has a protective effect on electrical sheet steel 20865 within a -0.2 to -0.05 V potential range and the presence of intermetallic FeAl and Fe_3Al phases degrades the magnetic properties of steel somewhat; the coercive force increases to 111.2 A/m and 110.4 A/m as a result of aluminizing for two and four hours, respectively. Figures 1; tables 1; references 1.

New High-Speed Flying Saws for Cutting Pipes and Roll-Formed Sections

927D0115D Moscow STAL in Russian No 1, Jan 92 pp 58-61

[Article by P. I. Sidorov, Yu. N. Bobylev, A. B. Lamin, Yu. N. Nabatov, V.N. Maslov, All-Union Scientific Research Institute of Metallurgical Machine-Building and Moscow Tube Plant; UDC 621.774.21]

[Abstract] The development of continuous electric tube welding machines for pipes of various cross sections and roll-formed sections necessitated the development of precise high-speed on-the-fly saws for cutting the tubes and sections into billets of a given length; the shortcomings of existing flying cutting machines are discussed, and the design of a new saw developed at the All-Union Scientific Research Institute of Metallurgical Machine-Building and Moscow Tube Plant is described. The tube movement cycle used in the new saw and the operating pie chart of the saw feed mechanism are plotted. A block diagram of the on-the-fly saw and a mechanical diagram of the 560M flying saw are cited. The saw disc performance is compared to that of the best foreign makes—the Clessime (France) and Mannesmann-Meer (Germany). Implementation of the new saw design makes it possible to make tubes and roll-formed sections of any shape in continuous bending and welding machines and to extend the service life of these machines as well as increase the cutting accuracy to within five mm. The use of the new saw reduces the volume of finishing operations. The specifications of the new saws exceed, or are comparable to, those of the best known foreign prototypes. Figures 4; tables 3.

Investigation of Cylindrical Screw Shell Rolling

927D0115E Moscow STAL in Russian No 1, Jan 92 pp 61-63

[Article by Yu. S. Zykov, O. V. Prilutskiy, Zaporozhye Industrial Institute and Kommunar Automotive Plant; UDC 621.771.6]

[Abstract] Flexible linkage cables encased in a cylindrical screw shell made by winding a flattened hardened wire in spring winding machines used in the automotive industry is discussed and a new method of making flexible cylindrical screw shells developed at the "Kommunar" Automotive Plant in Zaporozhye that combines the flattening and winding operations into one is outlined. The screw shells are rolled in a special unit equipped with a cantilever-mounted cylindrical roll with a flange and an eccentric ring. A rolling diagram of the cylindrical screw shell is cited and the dependence of the maximum possible percentage reduction on the diameter ratio of the roll and the eccentric ring and the dependence of the rolling force and the wire flattening factor on the roll/ring diameter ratio and the type of the blank are plotted. The combined reduction-winding process of making screw shells makes it possible to use less process equipment and requires less floor space for its implementation. The method also makes it possible to roll shell with a complex cross section shape, e.g., T-shaped and channel shaped. If the rolled blank is continuously straightened, the method may be efficiently used for making thin-walled sections in a single pass. Figures 3; references 5.

Effect of Vanadium on Failure Characteristics of High-Strength Steel Wire

927D0117A Moscow METALLOVEDENIYE I TERMICHESKAYA OBRABOTKA METALLOV in Russian No 9, Sep 91 pp 11-13

[Article by V. R. Baraz, A. A. Sokolov, Ye. A. Ishina, T. V. Golomazova, Urals Polytechnic Institute and All-Union Scientific Research Institute of Metalwares; UDC 621.778.0163:669.14.018]

[Abstract] The possibility of improving the properties of high-strength steel wire, produced by patenting with subsequent cold plastic deformation by drawing, by microalloying it with vanadium is investigated. To this end, the mechanical properties of carbon steel 70F of a close-to-eutectoid composition with 0.10 percent V are measured and compared for reference to those of standard carbon steel 70. The dependence of the ultimate rupture strength and limit of elasticity of steels 70F and 70 on the post-straining heating temperature, the effect of the post-straining heat treatment on the density and width of the B_{211} line, and the dependence of the austenite grain size of steels 70F and 70 on the austenization temperature are plotted. An analysis reveals that microalloying with 0.1 percent vanadium makes it possible to decrease steel 70's proclivity to delamination failure both after cold drawing and low-temperature tempering. The positive impact of vanadium is manifested, however, only after straining at a rather low reduction. If $\varepsilon > 80$ percent, the tendency to delamination may persist. This beneficial effect of vanadium is attributed to a decrease in the cementite decomposition rate during the drawing of patented wire and a decrease in the strain aging rate which affects the cracking severity. Figures 3; tables 1; references 3.

On Effect of Oxide Inclusions on Mechanical Properties of Steel With Low Carbon Content

927D0117B Moscow METALLOVEDENIYE I TERMICHESKAYA OBRABOTKA METALLOV in Russian No 9, Sep 91 pp 13-16

[Article by I. B. Gutovskiy, V. I. Bondarchuk, V. G. Kochkin, V. A. Kolchanov, Bolshevik Plant and Moscow Institute of Steel and Alloys; UDC 541.451:621.17:669.15-194]

[Abstract] The conventional view that nonmetallic inclusions always have a detrimental effect on the quality of steel is questioned; it is speculated that processes related to the formation of ternary and quaternary inclusions

significantly affect the quality of metal and the amount, dimensions, shape, and composition of nonmetallic inclusions. To check the hypothesis, two low carbon steel smeltings are analyzed; after melting, the metal is heated to a 1,630°C temperature and deoxidized by four methods using various amounts of Al, Mn+Si, Mn+Si+Al, and Si. The metals is then cast into ingots some of which are later forged. The study demonstrates that deoxidation with Si and Mn+Si leads to the formation of simple inclusions while deoxidation with Mn+Si+Al leads to complex inclusions; an increase in the oxygen concentration improves the metal's ductility, probably due to a decrease in its tendency to austenite grain growth. In the case where globular inclusions formed as a result of deoxidation with Si and Si+Mn+Al, an increase in the inclusion area also improves ductility since large inclusions do not serve as stress concentrators. On the other hand, deoxidation with Al and Si+Mn leads to a decrease in plasticity with an increase in the area of inclusions. Figures 1; tables 2; references 2: 1 Russian, 1 Western.

Heat Treatment of High-Speed Steel Tools Using High-Temperature Tempering

927D0118B Moscow METALLOVEDENIYE in Russian No 10, Oct 91 pp 6-7

[Article by I. K. Kupalova, Scientific Production Association of the All-Union Scientific Research Institute of Tools; UDC 669.14.018.252.3:621.785.796]

[Abstract] The shortcomings of multiple tempering with a mandatory cooling between the cycles are discussed and new high-temperature tempering methods developed at the Sestroretsk Tool Plant imeni Voskov, Orenburg Drill Plant, and Frunze Drill Plant and studied at the All-Union Scientific Research Institute of Tools are reported. Drills from steel R6M5 and R6M5K5 tempered by a two-cycle method are analyzed and recommendations are developed on this basis for the specific high-temperature tempering conditions of point tools from various brands of high-speed steel commonly used at today's toolmaking plants. The suggested conditions involve double tempering at temperatures of 570-600°C with a 10-36 min exposure. With respect to the tool properties attained, these conditions are equivalent to standard three-cycle tempering at 560°C with one hour cycles. It is noted that high-temperature tempering should be used only in computer-aided production lines for the heat treatment of tools in special attachments. Tables 1; references 20.

Improving Mechanical Properties of Steel 07Kh16N6 by Ausforming

927D0118C Moscow METALLOVEDENIYE in Russian No 10, Oct 91 pp 13-14

[Article by V. D. Afanasyev, G. A. Salishchev, K. G. Farkutdinov, Superplasticity Problems Institute at the USSR Academy of Sciences, Ufa; UDC 669.14.018.8:621.789]

[Abstract] The effect of the hardening temperature on the dissolution of coarse carbide is investigated and optimum ausforming conditions for producing a fine grain microstructure in steel 07Kh16N6 is determined. A comparative analysis of the structure and mechanical properties of austenitic-martensitic steel 07Kh16N6 after traditional treatment and thermomechanical ausforming is conducted, showing that the grain size decreases after ausforming while the strength and fracture resistance increase. Three treatment conditions are investigated: hardening at 1,00°C, hardening at 1,100°C, and hardening at 1,100°C with forging at 850 and 800°C and exposure to 800°C. An analysis reveals that thermomechanical treatment helps to dissolve coarse carbides and reduce the size of the initial austenite grain and makes it possible to improve the operating quality of steel. It is recommended that steel 07Kh16N6 be hardened at 1,100°C, isothermally forged at 850 and 800°C, cold-treated at a temperature below -70°C, and tempered at 425°C in order to increase its strength and toughness. Tables 1; references 8.

Effect of Superplastic Strain on Anisotropy of Steel 03Kh26N6T

927D0118D Moscow METALLOVEDENIYE in Russian No 10, Oct 91 pp 14-16

[Article by M. F. Ahmed Fouad, M. A. Tsepin, A. A. Lobach, Tabba Metallurgical Institute, Cairo, and Moscow Institute of Steel and Alloys; UDC 669.14.018.8:621.77]

[Abstract] The anisotropy patterns of corrosion-resistance steel 03Kh26N6T with an offset nonequiaxial fine grain structure after superplastic straining are considered and the dependence of the elongation of axial and radial samples on the initial straining rate and temperature, the dependence of the elongation anisotropy on the initial straining rate and temperature, and the dependence of the normal plastic anisotropy on the longitudinal strain at various sample temperatures are plotted. The relationship between the plastic anisotropy and the presence of initial metallographic irregularities in the steel structure is examined. An analysis of the findings shows that the maximum difference in the sample elongation along and across the rolling direction, given an optimum superplastic strain (SPD) temperature, does not fully characterize the steel anisotropy since it is due to the superplastic strain's elevated sensitivity to the transverse grain dimensions in these directions. The values of steel's 03Kh26N6T anisotropy indicator rise with the straining degree and temperature; this indicates that the anisotropy of steel's ductile properties decreases in the superplasticity condition. Figures 5; references 8: 6 Russian, 2 Western.

Properties of Microalloyed Boiler Steel After Controlled Rolling

927D0118E Moscow METALLOVEDENIYE in Russian No 10, Oct 91 pp 17-21

[Article by M. V. Bobylev, V. B. Kireyev, A. M. Koreshkova, Central Scientific Research Institute of Ferrous Metallurgy imeni I. P. Bardin; UDC 669.14.018.44:621.77]

[Abstract] The effect of microalloying with vanadium in the amount of 0.06 percent or niobium in the amount of 0.05 percent and controlled rolling with cooling in the air on the structure and structural strength level of carbon boiler steel 22K is investigated. Three ingots for the study are smelted in an induction furnace using the OZZhR burden, ferrovanadium, and metallic niobium; the ingots are then forged and control-rolled. The microstructure of the samples is examined under a scanning electron microscope and the dependence of the ferrite grain diameter on the rolling temperature, the dependence of the ferrite grain strain on the controlled rolling conditions, the dependence of the mechanical properties of the samples on the final rolling temperature, and the dependence of the long-term strength on the final controlled rolling temperature are plotted. An analysis of the curves and structural diagrams of the steels under study after controlled cooling demonstrates that controlled rolling makes it possible to increase the ultimate strength and long-term strength of steel; microadditions of vanadium and niobium magnify the effect by two-fold. Controlled rolling with subsequent controlled cooling helps to increase the ultimate strength of steel 22K by 1.3-1.5 times and that of microalloyed steel—by 2 to 3.5 times. An improved algorithm for calculating the thermomechanical treatment conditions is proposed. Figures 6; tables 1; references 8: 5 Russian, 3 Western.

Effect of Straining Temperature and Rate on Ductility of Alloy KhN62MBKTYu

927D0118F Moscow METALLOVEDENIYE in Russian No 10, Oct 91 pp 21-23

[Article by S. B. Maslenkov, I. V. Kabanov, Ye. A. Maslenkova, O. V. Abramov, I. N. Melkumov, Metallurgy Institute imeni A. A. Baykov; UDC 669.14.018.44:620.172:620.178.6]

[Abstract] The effect of the straining temperature and rate on the ductility of steel KhN62MBKTYu smelted in a vacuum induction furnace with subsequent vacuum arc refining and cooling in a mold is investigated. To this end, samples cut in a tangential direction from a forging made by upsetting are tested in an MTS tensile testing machine at a temperature of 950, 1,000, 1,050, 1,100, and 1,150°C with a broad range of straining rates from six to 5,000 mm/min. The structure of the fractured samples is analyzed and the dependence of the mechanical properties on the testing temperature, the grain size distribution in the initial state and after hot straining at various temperatures, and the dependence of the mean grain size on the straining rate at various temperatures are plotted. The results show that the strength of alloy KhN62MBKTYu may be increased at all temperatures within a 950-1,150°C range by increasing he straining rate from six to 4,000 mm/min yet an increase in the straining rate above 4,000 mm/min has virtually no effect on the alloy strength; the KhN62MBKTYu alloy ductility peaks at the dynamic recrystallization temperature. Straining at a six mm/min rate and a 1,150°C temperature facilitates dynamic poligonization which, in turn, increases ductility. The alloy fractures when strained at a temperature of 1,150°C at a 5,000 mm/min rate. The findings can be used to design optimum forging, extrusion, and rolling conditions. Figures 3; tables 2; references 3.

Production of Clad Metal Grey Cast Iron/Steel Joints by Forging and Explosion With Subsequent Thermal Cycling

927D0118H Moscow METALLOVEDENIYE in Russian No 10, Oct 91 pp 36-40

[Article by Yu. N. Taran, V. Ya. Slobodskoy, S. I. Gubenko, V. V. Sobolev, O. I. Konobritskaya, Dnepropetrovsk Metallurgical Institute and Dnepropetrovsk Mining Institute; UDC 62-419.4:669.014.018.298: 669.15-196]

[Abstract] The possibility of producing strong clad metal joints of grey cast iron with a ferrite or austenite matrix containing various modifications of graphite and carbon steel 40 is investigated. The microstructure of cast iron and steel is examined under a Neophot-21 microscope and with the help of an MS-46 X-ray spectral microanalyzer. The elementary processes occurring near the free contacting material surfaces during the forging, explosion, and thermal cycling and the element distributions are studied. It is shown that clad metal joints can be made by two methods: hot forging and a combination of explosion treatment with thermal cycling; there is almost no redistribution of the impurities and alloying elements during the forging and explosion while their effect during the thermal cycling is negligible. Production of this type of clad metal coats makes it possible to improve the mechanical and operating qualities of grey cast iron products and expand their applications in mechanical engineering. The mean grey cast iron hardness increases on the interface with steel from 105-108 H to 140-158 H. The principal shortcomings of the cast iron forging are eliminated in making clad metal. Figures 5; references 12.

Investigation of Mechanical Property Uniformity of VT9 Titanium Alloy Forgings After Superplastic Straining and Ausforming

927D0118J Moscow METALLOVEDENIYE in Russian No 10, Oct 91 pp 46-47

[Article by G.A. Salishchev, R.Ya. Lutfullin, M.A. Murzinova, Institute of Metal Superplasticity Problems at the USSR Academy of Sciences; UDC 669.295.5:621.7.043/ .044]

[Abstract] The mechanical properties and structure of the VT9 alloy after ausforming (VTMO) and superplastic straining (SPD) at varying degrees of reduction are investigated in order to identify the effect of the strain inhomogeneities in various cross sections of complex-shaped products on their mechanical properties. The grain size distribution in blanks made from a hot rolled bar and strained by flat dies is plotted. Metallographic studies are carried out using conventional procedures with a relative error of 7 percent and a confidence level of 90 percent. Mechanical tests are performed pursuant to GOST 1497—84. The study demonstrates that the strength and ductility of forgings from the VT9 alloy after superplastic straining with a 10-17 percent deformation are stable and remain adequate while both the micro- and macrostructure of these sample remain uniform. As the reduction degree increases, ausforming leads to a decrease in ductility and an increase in strength while the properties' spread is considerable; this is attributed to the structural inhomogeneity. Figures 1; tables 1; references 7.

Increasing Plate Steel Rolling Uniformity

927D0122D Moscow IZVESTIYA VYSSHIKH UCHEBNYKH ZAVEDENIY: CHERNAYA METALLURGIYA in Russian No 10, Oct 91 pp 23-25

[Article by M. Ya. Brovman, V. D. Dmitriyev, Kramatorsk Scientific Research and Design Institute of Mechanical Engineering; UDC 621.771.23]

[Abstract] The negative impact of plate thickness variation and the limited possibilities of resolving the problem by further increasing the stand stiffness by increasing the roll dimensions are discussed. The experimental dependence of the maximum finishing roll deformation of plate rolling mill 2300 on the rolling force for various plate strip widths is plotted and the roll sag function is analyzed. An analysis shows that the concave roll profile enhances the plate thickness variations while a new undulating roll shape is the most advantageous. The wave-shaped segments play a dominant role is preventing lateral plate displacements, i.e., ensure the rolling process stability; the results of 6,400 plate thickness measurements taken after rolling with new rolls are statistically summarized and the conclusion is drawn that the use of the wave-shaped roll profile in mill 2300 makes it possible to lower the transverse plate thickness variations by 1.5-2.0 times without capital outlays and results in saving more than 4,000 tons of steel and 320 thousand rubles per annum. Figures 2; tables 2; references 5.

Effect of Plastic Deformation, Ausforming, and Heat Treatment on Corrosion Behavior of Aluminum Alloyed With Rare Earth, Alkali, and Transition Metals

927D0122F Moscow IZVESTIYA VYSSHIKH UCHEBNYKH ZAVEDENIY: CHERNAYA METALLURGIYA in Russian No 10, Oct 91 pp 34-38

[Article by M. F. A. Fouad, Kh. Kurbanov, Moscow Institute of Steel and Alloys and Tabba Metallurgical Institute, Cairo; UDC 669.715.018.8:620.193:621.77.016]

[Abstract] The interaction of aluminum of varying degrees of purity with small alloying additions of rare earth and alkali earth elements and their effect on the corrosion resistance are discussed and a study of the corrosion behavior of samples produced by the joint smelting of alloy components in an SNVE-1-3-1/16 vacuum electric furnace and casting into cylindrical graphite molds are reported. The corrosion resistance of alloys is examined in a 3 percent NaCl solution by the potentiostatic method using a P5827M potentiostat and a PDP-4-002 XY-potentiometer. The chemical composition of the alloys and the sample treatment conditions—forging, broaching, and annealing—are summarized and typical potentiodynamic diagrams of aluminum alloys with Cu and Ce, anode potentiostatic curves of the Al-Mg-Mn-Ti-La-Ce alloys, and the dependence of the passivation current density on the passivation potential of cast and forged alloys are plotted. An analysis of the diagrams demonstrates that the corrosion resistance of the AmG3 T alloy in a neutral medium is very high, i.e., a current density is 0.01-0.08 A/cm_2, while the corrosion resistance of Al-Cu-Ce alloys is low in a neutral medium and satisfactory in an acid medium. Plastic deformation and ausforming decrease the corrosion resistance of all alloys while heat treatment increases it. It is shown that the optimum procedure for increasing the corrosion resistance of aluminum alloys is annealing and annealing with aging. The 5.0 alloy has the highest corrosion resistance in a neutral medium both in the cast and forged state. Figures 3; tables 7; references 10: 8 Russian, 2 Western.

Effect of Operating Parameters on Character of Structural Changes in Rotor Metal

927D0122H Moscow IZVESTIYA VYSSHIKH UCHEBNYKH ZAVEDENIY: CHERNAYA METALLURGIYA in Russian No 10, Oct 91 pp 55-56

[Article by V. P. Tarabanova, L. D. Mishchenko, T. M. Smolyakova, S. S. Dyachenko, Kharkov Automotive Engineering Institute; UDC 669.018.25:620.1]

[Abstract] A search for the possibility of extending the service life of rotors prompted a study of the character of the structural changes occurring in the metal during its operation; to this end, the metal of various rotor disc stages with 135,000 hours of service under various operating conditions at different temperatures is examined. The rotors are made from steel EI415. The microstructure of the rotor metal in the initial state and after 135,000 hours of operation is examined under an electron microscope and the grain size distribution in the disc metal is plotted. The study demonstrates that the bainite structure undergoes transformation during the disc operation; this is evident in the temperature-induced recrystallization activation and the grain boundary and subboundary migration; an X-ray structural analysis in a DRON-2 unit shows that carbide particles become isolated and coagulate, thus reducing the lattice constant. Stresses play a secondary role in activating the recrystallization processes. Figures 2; references 2.

Possibility of Developing Weldable Al-Cu-Li System-Based Alloys

927D0117G Moscow METALLOVEDENIYE I TERMICHESKAYA OBRABOTKA METALLOV in Russian No 9, Sep 91 pp 30-32

[Article by I. N. Fridlyander, A. M. Drits, T. V. Krymova, Scientific Production Association of the All-Union Aviations Materials Institute; UDC 620.179.2:669.715]

[Abstract] The inadequate level of the strength and ductility properties of welded joints from the VAD23 Al-Cu-Li alloy and its increased tendency to hot cracking prompted an examination of the weldability of a group of Al-Cu-Li alloys with 0.12 percent Zr on cold-rolled 2.5 mm thick sheets; the copper content in the alloy was varied within 1-5.5 percent and the lithium content—within 0-3 percent. The sheets were welded after a complete heat treatment cycle; the tendency to hot cracking was measured by the Moscow State Engineering University method. The dependence of the alloy weldability on the Cu and Li concentration, and effect of the Sc concentration on weldability, the HRC hardness behavior of the welded joint as a function of heat treatment after welding, and the mechanical properties on the testing temperature are plotted; the fractograms of the welded joints and the micro- and macrostructure of the welded joints are examined. The findings indicate two optimum Cu and Li concentration ranges from the viewpoint of weldability (5.5-6.5 percent Cu + 0.8-1.4 percent Li and 2.5-3.5 percent Cu + 1.9-2.5 percent Li) and reveal the positive effect of Sc on weldability and mechanical properties. A new 1460 alloy is developed as a result of the study; it has an adequate weldability without a filler while the use of an aluminum filler with 10 percent Cu considerably lowers its tendency to hot cracking. Figures 6; tables 2; references 7: 5 Russian, 2 Western.

Promising Friction Welding Methods

927D0125A Moscow SVAROCHNOYE PROIZVODSTVO in Russian No 10 (684), Oct 91 pp 2-3

[Article by E. S. Karakozov, V. I. Yegorov, V. I. Dyachenko, Ye. T. Puteyev, V. N. Kashcheyev, E. L. Volf, Remdetal All-Union Scientific Production Association, Scientific Production Association of the Altay Scientific Research Institute of Machine Building Technology, Minsk Tractor Plant, and Tomsk Polytechnic Institute; UDC 621.791.01"313"]

[Abstract] The principal parameters of friction welding—the pressure in the heating phase, the upset forging pressure, the heating duration, the upset forging duration, and the rotation speed—are summarized and the new promising methods of friction welding, such as welding without upset-forging the pieces together and combined welding with self-control of the friction process in the shock mode, are investigated. The microstructure of nickel and nickel plus copper welds is examined and the design of the upgraded SMTS-74 friction welding unit and its operation are described. The unit has the following specifications: a welding output of up to 180 per hour, a power rating of 6.5 kW, an axial force of 50 kN, and overall dimensions of 2,230x1,360x1,525 mm. The principal advantages of the new method include a higher weld quality for materials which generally have poor weldability, a smaller welding allowance, and a lower power consumption. Figures 2; tables 1; references 5.

High-Temperature Brazing of Steel With Wide Gap

927D0125B Moscow SVAROCHNOYE PROIZVODSTVO in Russian No 10 (684), Oct 91 pp 7-10

[Article by V. N. Radziyevskiy, V. L. Dudchenko, G. G. Tkachenko, All Union Scientific Research Institute of Compressor Building; UDC 621.791.3.05.011:539.2]

[Abstract] The negative effect of the brazing gap size on the mechanical properties of the brazed joint is discussed and a method of increasing the gap without decreasing the quality of the hot-brazed joint on steel is examined. Using a certain combination of filler and brazing solder components, it is possible even to improve the joint quality; in some cases the carbon steel joint toughness reaches that of the base steel. The causes of the improvement in the mechanical properties, which open up new possibilities of improving the quality of brazed joints, are investigated. To this end, the effect of the gap width on the toughness of a joint brazed with a Cu-Mn brazing solder and Fe-Ni filler and the effect of the gap width on the toughness of a steel 20 joint brazed with a Cu-Mn solder and Fe-Ni filler are plotted. The microstructure of the brazed joint made with various fillers is examined. A study of various types of joints and their properties indicates that with certain combinations of solders and fillers, deliberately wide gaps expand applications of the hot brazing method and make it possible to produce high-quality joints in poorly accessible locations. Figures 7; tables 4; references 9.

Assessing Base Metal and Welded Joint Quality of Variable-Composition Alloys

927D0125C Moscow SVAROCHNOYE PROIZVODSTVO in Russian No 10 (684), Oct 91 pp 14-17

[Article by A. V. Surkov, Yu. I. Baryshnikov, P. N. Kipiani, N. A. Talanova, V. I. Panov, Scientific Production Association of the Central Scientific Research Institute of Mechanical Engineering Technology and the Uralmash Production Association; UDC 621.791.052:620.18]

[Abstract] The need to assess the minimum guaranteed level of mechanical properties for content variations within the range specified by the brand when new brands of steel and alloys are introduced and the difficulty of smelting steel with the specified concentrations of alloying components are identified. The minimum warranted properties of steel 12KhGN3MFAYuDR-Sh and its welded joints produced by carbon dioxide welding with PP-AN57 and Sv-09G2S electrode wires are evaluated. The alloying element concentration in steel is cited and the alloying element and alloying degree distribution, the dependence of the base metal strength and ductility on the alloying degree, the relationship between hardness and ultimate strength and yield strength and between hardness and elongation and reduction of area, the hardness and yield strength behavior of the variable-composition metal as a function of the tempering exposure length, the dependence of toughness behavior on the alloying degree, and the ultimate strength of welded joints as a function of the alloying degree after tempering are plotted. The microstructure of steel 12KhGN3MFAYuDR-Sh with varying degrees of alloying after the principal heat treatment is examined. An analysis demonstrates that variable-composition alloys make it possible to determine the minimum guaranteed level of the base metal's and welded joint's mechanical properties efficiently and with high confidence and shows that the RU 14-1-4145—86 requirements for the ultimate strength and yield of steel 12KhGN3MFAYuDR are met only at a >0.29 alloying degree but the elongation requirements are not met at this level. Figures 8; tables 1; references 4.

Selection Criteria of Tools for Ultrasonic Welding of Element Leads on Polyimide Board

927D0125D Moscow SVAROCHNOYE PROIZVODSTVO in Russian No 10 (684), Oct 91 pp 24-27

[Article by V. G. Podlesnykh, M. A. Tkachev, V. A. Zelenov, V. I. Titov, Moscow State Electronic Engineering Institute; UDC 621.791.16.03:621.382]

[Abstract] The advantages of hybrid integrated circuits and chips on a polyimide board with elements which are not encased in a package are discussed and the criteria for selecting the tools for ultrasonic welding of these elements' leads are investigated. The effect of the tool vibration on the welded joint quality is examined and the design peak-to-peak amplitude of the vibrating tool's longitudinal axis, the dependence of the relative tool vibration amplitude on its protrusion, and the dependence of the relative vibration amplitude and welded joint strength on the protrusion of the cross-type tool without a tail piece are plotted. The working end of the cross- and capillary-type welding tool after welding 500 spots is examined under a microscope. The study makes it possible to formulate the criteria for selecting the tools for ultrasonic welding of aluminum band leads; the main requirement is that the joints have equal strength with the leads and that the tool's weld tack be stable. The optimum results are attained by using the capillary-type tool with a 150 μm working end diameter for 300 μm wide leads and a protrusion of less than seven mm, i.e., less than the resonant length, and without a tail section. Figures 4; tables 2; references 6.

Micrometering Soldering Pastes for Computer-Aided Microelectronics Product Assembly Process

927D0125E Moscow SVAROCHNOYE PROIZVODSTVO in Russian No 10 (684), Oct 91 pp 32-33

[Article by A. I. Galushka, A. A. Rossoshinskiy, P. Ye. Kandyba, I. L. Novak, Branch No 2 of the Scientific Research Institute of Retail Trade and Food Service, Electric Welding Institute imeni Ye. O. Paton, Fonon Scientific Research Institute, and Computer Science Institute at the Ukrainian Academy of Sciences; UDC 621.791.303-52:658.527]

[Abstract] The need to improve the microsoldering quality and reduce the effect of the human factor prompted efforts to automate the micrometering of soldering pastes—one of the main operations in assembling the microelectronic products by soldering; consequently, the effect of the rheological properties of soldering pastes (PP) and the geometric dimensions of the metering unit on the micrometering process is investigated. To this end, a mathematical model of the micrometering process is constructed and theoretical and experimental studies are carried out. The dependence of the soldering paste microbatch on the rheological constants and the dependence of the soldering paste flow rate (by mass) on the pressure magnitude and application duration are plotted and a schematic drawing of the metering unit is cited. The resulting experimental and analytical data are used to design the processes and equipment as well as a computer program for controlling the micrometering process during the automated precision soldering of piezoelectronic components. The following optimum process parameters are established for obtaining microbatches of two to 10 mg: a metering nozzle diameter and height of five and 50 mm, respectively; a needle diameter of ≤0.8 mm for soldering pastes with a ≤40 μm particle size; a pressure drop of ≤0.25 MPa; a batching pulse duration of ≤2.5 s. Figures 3.

Hydrogen Diffusion During and After Electron Beam Welding of Titanium Alloys

927D0125F Moscow SVAROCHNOYE PROIZVODSTVO in Russian No 10 (684), Oct 91 pp 39-41

[Article by A. V. Fishgoyt, B. A. Kolachev, A. A. Mamayev, Yu. M. Shtemler, Central Scientific Research Institute of Aviation Engine-Building imeni L. I. Baranov, Moscow Aviation Engineering Institute imeni K. E.

Tsiolkovskiy, and Scientific Production Aviation Association imeni A. N. Tupolev; UDC 621.791.72:621.78.669.295]

[Abstract] The hydrogen mass transfer process both during the electron beam welding (ELS) of titanium alloys and after their welded joint exposure to 18-20°C for an extended time is investigated. It is assumed that the mass transfer process during the welding occurs as a result of diffusion under the effect of temperature gradients or the hydrodynamics of the molten metal; the convective component is ignored due to the metal's high viscosity. After the welding, hydrogen diffusion is assumed to occur under the effect of the residual stress gradients and the differences in the phase composition in the welded joint segments. A physical-mathematical process model is derived and the heat transfer equation is solved. The β-phase distribution in the VT6 alloy after electron beam welding, the stress component distribution in VT6 alloy joint, the design hydrogen distribution in the weldpool in front of and behind the weld, and the hydrogen concentration distribution immediately after welding of a Ti-6Al-4V alloy are plotted. The experiments show that during the storage of welded joints, hydrogen is redistributed due to diffusion to the tensile stress areas and areas with an elevated β-phase concentration. An analysis of the physical and mathematical models describing the convective and diffusive hydrogen redistribution along and across the welded joint during and after electron beam welding confirms the consistency of the theoretical data with the experimental results. The authors are grateful to T. V. Ivanova, I. D. Nizkin, and S. P. Belov for help with experiments. Figures 6; references 9: 7 Russian, 2 Western.

NTIS
ATTN PROCESS 103
5285 PORT ROYAL RD
SPRINGFIELD VA 22161

Foreign Broadcast Information Service (FBIS) and Joint Publications Research Service (JPRS) publications contain political, military, economic, environmental, and sociological news, commentary, and other information, as well as scientific and technical data and reports. All information has been obtained from foreign radio and television broadcasts, news agency transmissions, newspapers, books, and periodicals. Items generally are processed from the first or best available sources. It should not be inferred that they have been disseminated only in the medium, in the language, or to the area indicated. Items from foreign language sources are translated; those from English-language sources are transcribed. Except for excluding certain diacritics, FBIS renders personal names and place-names in accordance with the romanization systems approved for U.S. Government publications by the U.S. Board of Geographic Names.

Headlines, editorial reports, and material enclosed in brackets [ ] are supplied by FBIS/JPRS. Processing indicators such as [Text] or [Excerpts] in the first line of each item indicate how the information was processed from the original. Unfamiliar names rendered phonetically are enclosed in parentheses. Words or names preceded by a question mark and enclosed in parentheses were not clear from the original source but have been supplied as appropriate to the context. Other unattributed parenthetical notes within the body of an item originate with the source. Times within items are as given by the source. Passages in boldface or italics are as published.

SUBSCRIPTION/PROCUREMENT INFORMATION

The FBIS DAILY REPORT contains current news and information and is published Monday through Friday in eight volumes: China, East Europe, Central Eurasia, East Asia, Near East & South Asia, Sub-Saharan Africa, Latin America, and West Europe. Supplements to the DAILY REPORTs may also be available periodically and will be distributed to regular DAILY REPORT subscribers. JPRS publications, which include approximately 50 regional, worldwide, and topical reports, generally contain less time-sensitive information and are published periodically.

Current DAILY REPORTs and JPRS publications are listed in *Government Reports Announcements* issued semimonthly by the National Technical Information Service (NTIS), 5285 Port Royal Road, Springfield, Virginia 22161 and the *Monthly Catalog of U.S. Government Publications* issued by the Superintendent of Documents, U.S. Government Printing Office, Washington, D.C. 20402.

The public may subscribe to either hardcover or microfiche versions of the DAILY REPORTs and JPRS publications through NTIS at the above address or by calling (703) 487-4630. Subscription rates will be provided by NTIS upon request. Subscriptions are available outside the United States from NTIS or appointed foreign dealers. New subscribers should expect a 30-day delay in receipt of the first issue.

U.S. Government offices may obtain subscriptions to the DAILY REPORTs or JPRS publications (hardcover or microfiche) at no charge through their sponsoring organizations. For additional information or assistance, call FBIS, (202) 338-6735,or write to P.O. Box 2604, Washington, D.C. 20013. Department of Defense consumers are required to submit requests through appropriate command validation channels to DIA, RTS-2C, Washington, D.C. 20301. (Telephone: (202) 373-3771, Autovon: 243-3771.)

Back issues or single copies of the DAILY REPORTs and JPRS publications are not available. Both the DAILY REPORTs and the JPRS publications are on file for public reference at the Library of Congress and at many Federal Depository Libraries. Reference copies may also be seen at many public and university libraries throughout the United States.